NASA TECHNICAL NOTE

NASA TN D-6230

A TECHNIQUE FOR EVALUATING PARAMETER VARIATIONS FOR AUTOMATICALLY CONTROLLED AIRCRAFT WITH AN APPLICATION TO THE LANDING APPROACH

by Stuart C. Brown and Homer Q. Lee

Ames Research Center
Moffett Field, Calif. 94035

NATIONAL AERONAUTICS AND SPACE ADMINISTRATION • WASHINGTON, D. C. • MARCH 1971

1. Report No.	2. Government Accession No.	3. Recipient's Catalog No.
NASA TN D-6230		

4. Title and Subtitle

A TECHNIQUE FOR EVALUATING PARAMETER VARIATIONS FOR AUTOMATICALLY CONTROLLED AIRCRAFT WITH AN APPLICATION TO THE LANDING APPROACH

5. Report Date: March 1971

6. Performing Organization Code:

7. Author(s): Stuart C. Brown and Homer Q. Lee

8. Performing Organization Report No.: A-3244

9. Performing Organization Name and Address:
NASA Ames Research Center
Moffett Field, Calif. 94035

10. Work Unit No.: 125-19-03-15-00-21

11. Contract or Grant No.:

12. Sponsoring Agency Name and Address:
National Aeronautics and Space Administration
Washington, D. C. 20546

13. Type of Report and Period Covered: Technical Note

14. Sponsoring Agency Code:

15. Supplementary Notes:

16. Abstract

A method involving the minimization of a performance criterion was used to analyze the ability of automatically controlled aircraft to maintain accurate flight-path control during the landing approach. The criterion was based primarily on the ability of the aircraft to follow a constant slope glide path in the presence of statistically described gust disturbances. Constraints on the adjustments of the linear control system parameters were included as part of the method. The method was implemented by means of a digital computer to perform the parameter search required for the minimization of the performance index. The utility of the method was evaluated by determining effects of variations in several aircraft parameters on the control of longitudinal motions of a subsonic and a supersonic jet transport aircraft.

17. Key Words (Suggested by Author(s))	18. Distribution Statement
Automatic landing control Aircraft control Feedback control Flight control Optimization	Unclassified – Unlimited

19. Security Classif. (of this report)	20. Security Classif. (of this page)	21. No. of Pages	22. Price*
Unclassified	Unclassified	47	$3.00

*For sale by the National Technical Information Service, Springfield, Virginia 22151

CONTENTS

NOTATION

A,B,C	constant coefficient matrices describing effects of state, control, and disturbance variables in equations of motion
C_D	drag coefficient, drag/qS
C_L	lift coefficient, lift/qS
C_m	pitching-moment coefficient, pitching moment/qSc
c	longitudinal reference length
E( )	expected, or average, value of the quantity indicated in brackets
H	augmented performance function
h	altitude deviations from desired flight path
I	identity matrix
I_y	pitching moment of inertia
J	performance index
j	imaginary part of complex quantity
K	feedback gain matrix of state variables
K_v	feedback gain matrix of barometric variables
k_{ij}	feedback gain of state variable j into control variable u_i
L_u, L_w	gust scale lengths for horizontal and vertical gusts, respectively
M_{δ_t}	pitching acceleration due to engine thrust change
m	aircraft mass
P,Q	weighting matrices in performance index
q	dynamic pressure, $(1/2)\rho U_o^2$
S	wing reference area
s	Laplace transform variable

U_o	steady-state forward velocity of aircraft
u,w	perturbation velocities along horizontal and vertical stability axes
$\underline{u}_c$	control variable vector
u_g, w_g	horizontal and vertical gust disturbance velocities
u_{δ_e}	control variable for elevator control
u_{δ_t}	control variable for throttle control
V_s	aircraft stall velocity
$\underline{v}$	disturbance velocity vector
X_{δ_t}	acceleration in direction of horizontal stability axis due to engine thrust change
$\underline{x}$	state variable vector
x_v	aircraft velocity portion of aircraft state vector
Z_{δ_t}	acceleration in direction of vertical stability axis due to engine thrust change
α	angle of attack
γ	closed-loop pole
γ_o	steady-state glide-path angle
δ_e	elevator angle deviation from steady state, positive, t.e., downward, radians
δ_t	thrust deviation from steady state, kilopounds
ζ	damping ratio
θ	incremental aircraft pitch angle
λ	penalty function constant
ρ	density of air
σ_i	root mean square of the quantity, i
σ_g^2	normalized mean square gust disturbance used in calculations [$\sigma^2_{w_g} = 1$ $(fps)^2$, $\sigma^2_{u_g} = (3/2)(fps)^2$]
τ_e	elevator servo time constant

τ_t	engine control time constant
Φ	power spectral density function
ϕ	correlation function
ω_n	undamped natural frequency
$\Re$	real part of complex quantity
$(\dot{})$	differentiation with respect to time

Aircraft Stability Derivatives

$$C_{D_\alpha} = \frac{\partial C_D}{\partial \alpha} \qquad C_{L_{\dot{\alpha}}} = \frac{\partial C_L}{\partial (\dot{\alpha} c/2U_o)} \qquad C_{m_\alpha} = \frac{\partial C_m}{\partial \alpha}$$

$$C_{L_q} = \frac{\partial C_L}{\partial (\dot{\theta} c/2U_o)} \qquad C_{L_{\delta_e}} = \frac{\partial C_L}{\partial \delta_e} \qquad C_{m_{\dot{\alpha}}} = \frac{\partial C_m}{\partial (\dot{\alpha} c/2U_o)}$$

$$C_{L_\alpha} = \frac{\partial C_L}{\partial \alpha} \qquad C_{m_q} = \frac{\partial C_m}{\partial (\dot{\theta} c/2U_o)} \qquad C_{m_{\delta_e}} = \frac{\partial C_m}{\partial \delta_e}$$

Subscripts

ℓim	limit value of pole
max	magnitude of gain constraint
o	steady-state value
s	stall value

Matrix Operations

-1	inverse of matrix
t	transpose of matrix

A TECHNIQUE FOR EVALUATING PARAMETER VARIATIONS FOR AUTOMATICALLY CONTROLLED AIRCRAFT WITH AN APPLICATION TO THE LANDING APPROACH

Stuart C. Brown and Homer Q. Lee

Ames Research Center

SUMMARY

A method based on the minimization of a performance criterion was used to analyze the effects of several aircraft parameters on the ability of automatically controlled aircraft to maintain accurate flight-path control during the landing approach. The criterion was based primarily on the ability of the aircraft to follow a constant slope glide path in the presence of statistically described gust disturbances. The optimum performance for a flight condition was determined by adjusting the linear control system parameters to minimize the performance criterion. The method incorporated constraints on the adjustment of control system parameters; these constraints consisted of limiting the magnitudes of the control system gains and also degree of stability constraints in the form of restrictions on the damping characteristics of the closed-loop poles. The adjustments were implemented by means of a digital computer for a numerical search procedure and evaluation of the performance index.

To evaluate the method, effects of variations in several aircraft parameters on the control of longitudinal motions of a subsonic and a supersonic jet transport aircraft were investigated. The selection of coefficients for the criterion emphasized the reduction of altitude errors. The combined use of elevator and throttle controls was included. Examination of one parameter, the nominal approach velocity for a typical subsonic transport, revealed considerable deterioration in performance as the approach velocity decreased. Some effects of control system feedback parameters were also evaluated. Inertially measured vertical velocity signals were shown to be more effective than barometrically measured vertical velocity (angle of attack) signals for control in the presence of gust disturbances. The performance of a system controlling a large transport designed for supersonic speeds was determined to be poorer than that achieved for the smaller subsonic transport. Effects on the supersonic transport of different longitudinal control surface locations were investigated, and tradeoffs in control performance between surfaces with varying amounts of assumed aerodynamic lift and moment effectiveness were determined.

INTRODUCTION

Increasing numbers of automatic functions are being incorporated into control systems for high-performance aircraft to meet the performance requirements of all-weather landing systems (ref. 1). In the design of an automatic system, a necessary objective is to select as explicit a design or performance criterion as possible to permit synthesis of the control system and to evaluate the

resulting overall performance. This selection becomes more difficult when multivariable aspects of the system are included, and a suitable overall response through the use of several control inputs must be obtained. In addition, the criterion should be applicable to the evaluation of effects of changes in both control system and aircraft parameters.

The performance index used in linear optimal control theory provides an attractive criterion for determining and evaluating multivariable linear control systems (refs. 2 and 3). This scalar index is a time integral of a quadratic function of the system variables. To use the criterion, suitable coefficients for the performance index must be selected. The theory then provides a direct means for determining those feedback gains that minimize the performance index for response to arbitrary initial conditions, as well as for certain disturbance functions as long as no constraints on the system are considered. With constraints added to the formulation of the problem, the combination of control system gains that minimizes a performance index, and hence the resulting system, depends on the particular initial condition or disturbance function used. One form of constraint is to restrict the magnitude of the control gains. In reference 4, for example, the control gains were adjusted within a selected range to minimize a performance index that was evaluated on the basis of system response to an initial condition. Gain constraints are often needed since the control signals of an automatic system may be purposely restricted so that the pilot can manually override them if necessary, or the likelihood of control saturation can be reduced. Moreover, only certain feedback variables may be available.

Another form of control performance criterion is to prescribe particular pole locations for the closed-loop system (*e.g.*, ref. 5); additional specifications generally must be included to determine the control system uniquely, and these depend on the order of the system relative to the number of poles specified and also on the number of control inputs. Specifications relating to certain zero's of the closed-loop system were used in reference 5.

The purposes of this report are: (1) to present a technique for the synthesis and evaluation of a system by means of a proposed performance criterion, which consists of the minimization of a performance index subject to two types of constraints; and (2) to demonstrate the utility of the criterion, for determining effects of changes in various parameters on control performance. The first type of constraint is a restriction on the magnitudes of the feedback gains. The second type relates to the transient behavior of the controlled system. This constraint consists of restrictions on the poles of the closed-loop system to certain regions. The performance index to be minimized subject to the constraints is based on the response of the automatically controlled aircraft to a statistically described disturbance. This resulting criterion represents a somewhat different combination of performance index minimization in the presence of constraints than those considered previously.

One application of the technique would be for a nominal flight condition and set of aircraft parameters to determine the control parameters and the resulting system performance. The performance of this control system then would be evaluated further by determining changes in the performance index due to changes in various aircraft parameters. Another application of the technique which will be used in the present report is intended to show more clearly the effects of changes in aircraft parameters on the automatically controlled aircraft through use of the performance criterion. In this application, as an aircraft parameter is changed, a new set of gains that minimize the performance criterion is determined, together with the corresponding value of best performance. Thus, effects of variations in aircraft parameters are compared through the use of an explicitly expressed control performance criterion, which includes a constrained level of control

effort as the parameters are varied. This means of comparing effects for an automatic system is somewhat similar to the extensively used pilot opinion evaluations of variations in aircraft parameters for manually controlled systems (ref. 6).

Thus, the technique provides a means for quantifying tradeoffs between aircraft parameters in terms of the performance of the automatic system optimized for each set of parameters. To demonstrate this use of the method, some examples are given that show effects of several parameters on the control performance of transport aircraft during the landing approach. In these examples, parameters for the performance criterion were selected, and the criterion was used to evaluate the ability of an automatically controlled aircraft to follow a desired constant glide path in the presence of a statistically described gust disturbance. Only control aspects of the problem were investigated in that no attempt was made to account for effects of imperfect measurements of the states.

ANALYSIS

The procedure for synthesizing a control system and evaluating the controlled aircraft performance is described in this section. The performance is based on the ability of an automatically controlled aircraft to follow closely a constant flight path in the presence of gust disturbances. A scalar performance index based on the aircraft response is used. The control system is determined through use of a performance criterion which consists of the minimization of a performance index subject to several constraints on the adjustment of the control system parameters. This value of the performance index is then used as a measure of control performance. Multivariable aspects of the problem are considered in that interacting effects of pertinent control and state variables are included. One objective of the criterion is that it be useful for evaluating effects of changes in several aircraft characteristics on the ability to control the aircraft. While the method can be applied to other aircraft control problems, the description that follows will be oriented toward an application to aircraft landing approaches. Only control aspects of the problem will be investigated; a more complete analysis of automatic system performance would include a determination of filtering requirements to reduce effects of measurement errors.

Performance Criterion

The performance criterion selected and the principal assumptions used in the analysis are described in this section. The analysis is based on an evaluation of the ability of an automatically controlled aircraft to follow a nominal flight path with a constant forward velocity in the presence of gust disturbances. The disturbances are described by linear stationary statistics. The resulting aircraft motions about the nominal flight path also can be described by linear stationary statistical averages (variances) and are used for evaluating the controlled aircraft performance.

Equations of motion– For the determination of the statistical averages, the aircraft motions are assumed sufficiently small that they can be described by linear differential equations with constant coefficients. Equations representing aircraft control surface dynamics and engine response are also assumed to be of the same form. For the subsequent examples, only the equations describing motions of the aircraft in the vertical plane will be used. These equations were obtained

by summation of horizontal and vertical forces and pitching moments, with the state variables expressed in the stability axis system. An additional linearized equation expressed the kinematic relation for obtaining vertical velocity perpendicular to the nominal flight path. Equations for elevator and throttle controls included first-order control dynamics. A detailed description of the equations used for the cases to be investigated is given in appendix A.

For evaluation, the linearized aircraft equations of motion, together with the control system dynamics, are arranged into the following first-order constant-coefficient matrix form:

$$\dot{\underline{x}} = A\underline{x} + B\underline{u}_C + C\underline{v} \tag{1}$$

These equations represent the variations in the state variables $\underline{x}$ that are caused by the control variables $\underline{u}_C$ and the disturbance velocity variables $\underline{v}$. The $\underline{x}$ and $\underline{v}$ vectors represent motions of the aircraft and wind gusts relative to the fixed reference flight-path trajectory; expressions for the A, B, and C matrices for the longitudinal case are given in appendix A.

To form the closed-loop system, the feedback signal to each control variable $\underline{u}_C$ is assumed to be a linear combination of the selected measured variables. It is convenient to separate these variables into the two forms indicated in equation (2).

$$\underline{u}_C = -K\underline{x} - K_V(\underline{x}_V - \underline{v}) \tag{2}$$

The principal quantities measured are the state variables $\underline{x}$, which include aircraft velocities defined relative to an inertially fixed reference flight path. The additional feedback quantity indicated by equation (2) represents a velocity measurement defined as the difference between the aircraft inertial velocity $\underline{x}_V$ and the wind disturbance velocity $\underline{v}$. This form of measurement will be referred to as a "barometric measurement." The differential equations of motion for the closed-loop system are obtained by substituting equation (2) into equation (1), giving

$$\dot{\underline{x}} = (A - BK)\underline{x} - BK_V(\underline{x}_V - \underline{v}) + C\underline{v} \tag{3}$$

Performance index— The performance index to be minimized is determined from the aircraft response to the disturbance $\underline{v}$. The disturbance is described by linear steady-state statistics, and since the equations of motion are linear, the vehicle response can be determined by using time-averaged values or steady-state covariances of the states. To provide a meaningful measure of performance along the flight path, a performance index is selected in the form of a linear combination of covariances of state variables plus the barometrically determined variables:

$$J = E(\underline{x}^tQ\underline{x}) + E[(\underline{x}_V - \underline{v})^tP(\underline{x}_V - \underline{v})] \tag{4}$$

The covariances of these variables represent averages of products of deviations from nominal values for the reference flight path, and their relative weightings are given by the Q and P matrices. The barometric variables are included in the performance index, since a portion of the control task, in addition to providing flight-path control, is to reduce these variables to suitable magnitudes. The method used to evaluate the performance index for a preselected set of control gains (which then specifies all quantities in eq. (3) since the aircraft parameters are already known), is given in

appendix B. The desired control system is synthesized and the performance evaluated by a search procedure to determine the set of gains that minimizes the performance index (eq. (4)) subject to certain constraints described below. For this investigation, no separate weighting factors for the control variables $\underline{u}_c$ were considered necessary for the performance index, since the constraints were believed to delineate more clearly the limitations on control effort.

Constraints– Two forms of constraints are used on the range of gain adjustments. The first are limits on the magnitudes of the state and the barometric feedback gains; these limits are represented symbolically by

$$\left.\begin{aligned} |K| &\leqslant K_{max} \\ |K_V| &\leqslant K_{V_{max}} \end{aligned}\right\} \tag{5}$$

These constraints provide a means for reducing the likelihood of saturation of the controls. In addition, an adjustment in the value of the gain constraint for a particular variable provides a means for determining the importance of the variable as a control signal. Moreover, the use of some state variables as feedback signals may not be feasible. For instance, control dynamics such as elevator actuator dynamics often must be considered invariant because of weight and power restrictions. Hence, feedback gain around a control representation that results in higher frequency control dynamics cannot be considered. A control gain also may be restricted because of the poor quality of the measured information, or because elaborate measurements and filtering would be required to provide a usable signal in the control frequency range. Another reason for restricting control gains is to avoid the excitation of structural modes without having to resort to a more complex design, which might have less tolerance for changes in system parameters.

The second form of constraint on the adjustment of system gains is the restriction of the poles of the closed-loop system to a predetermined region of the complex plane. In some cases, it may be satisfactory to select specific closed-loop poles; in general, however, it is believed better to specify only a pole region and combine this specification with minimization of the performance index. The allowable pole region is defined by the boundaries

$$\left.\begin{aligned} \Re(\gamma) &\leqslant \Re_{\ell im} \\ \zeta(\gamma) &\geqslant \zeta_{\ell im} \end{aligned}\right\} \tag{6}$$

With this form of constraint, some dynamic considerations can be introduced in addition to that provided by the response to the disturbance. The constraint on damping ratio $\zeta_{\ell im}$ represents a specification of the relative stability of the system. The constraint on the real part of the poles $\Re_{\ell im}$ is a means of ensuring that the closed-loop response will approach, and the statistical averages will reach steady-state values within a certain time interval. It should be noted that separate specifications of pole and gain constraints may not be compatible; in such cases some compromise in selection may be needed.

Synthesis Procedure

The control system is determined by the set of control gains that results in a minimization of the performance index (eq. (4)). The performance is computed by the differential equation describing the deviations from the flight path that result from a selected random disturbance (eq. (3)). Constraints on magnitudes of the gains (eqs. (5)) and on locations of the closed-loop poles (eqs. (6)) must be satisfied. The presence of the constraints precludes the use of any available analytical method to solve directly for the control system gains. A numerical search procedure, utilizing a digital computer, is used to determine the set of gains for which J is a minimum and the constraints are satisfied. A single step in the procedure is to select a set of gains and then compute the resulting closed-loop poles and performance index. A residue method (appendix B) is used to determine the performance index from the preselected set of gains. The output state variables are first expressed in a matrix, frequency domain (spectral) form as a function of the disturbance variables and the equations of motion relating the output and disturbance variables. The poles of the closed-loop system are determined, and the frequency domain form is expanded by the method of residues to obtain the covariance matrix of the output variables. The performance index is then calculated from the covariance matrix and weighting matrices. In the formulation of the method for the computer, provision must be made for the various combinations of complex and real poles that occur for the closed-loop system of interest. A subsequent set of gains is obtained from the search procedure by a comparison of the present value of the performance index with those from previous computations. For the examples investigated, at least one closed-loop complex pole pair is driven toward the damping ratio constraint boundary.

An automated search procedure requires a method that searches along one or more pole constraint boundaries to obtain the minimum value of the performance index that can be achieved within the allowable range of gains. An available computer optimization program (ref. 7) was adapted to these computations. The program contains several search algorithms for minimizing a multivariable function, and includes provisions for constraints on magnitudes of the independent (control) variables. In addition, provision is made for including equality constraint functions of variables by constructing an augmented function to be minimized, which is obtained by adding a quadratic function of the equality constraints to the original function.

For the present analysis, the constraint function included in the computations is the damping ratio portion of the pole constraint (eqs. (6)). This constraint was added to the performance index to form the following augmented performance function

$$\left.\begin{aligned} H(K) &= J(K) + \sum_i \lambda_i [\zeta_i(K) - \zeta_i]^2 \qquad \text{for} \quad \zeta_i < \zeta_{\ell im} \\ H(K) &= J(K) \qquad \text{for} \quad \zeta_i \geqslant \zeta_{\ell im} \end{aligned}\right\} \tag{7}$$

The subscript i denotes different complex conjugate pole pairs for the closed-loop system. It will be noted that the penalty function added is of unsymmetrical form since an inequality constraint is being included.

The remaining parameters to be specified in equations (7) are the penalty function constants λ_i. The selection of these constants involves a compromise that can be established only through several trial calculations. The constants must be sufficiently large that the constraints are

satisfied to an adequate degree of accuracy when the minimum value of the performance function is obtained. On the other hand, large values of the constants will retard convergence since hillsides have been added to the performance index surface by the unsymmetrical constraint functions. Hence, the relatively smooth surface J has been changed to a more irregular one H.

The particular search algorithm selected from the optimization program (ref. 7) was the "adaptive creeper," which appeared to provide reasonable efficiency in searching near the constraint boundaries and required a minimum of additional calculations. The procedure consists of incrementing a control variable by a preselected amount and determining whether performance improves. Succeeding increments of this variable are increased if performance improves or decreased if performance does not improve after perturbing the variable in both directions. The procedure is repeated for each control variable, and the entire cycle is repeated until a minimum value of sufficient accuracy is achieved.

The overall search procedure included several steps. Certain gains, previously determined to have primary effects on the performance index, were adjusted to be as large as possible and still meet the constraints on the closed-loop poles and gains. This step ensured establishment of a proper pole pattern compatible with the performance index calculation described in appendix B. Thus, the range of gains to be searched by the performance index computation was reduced to moderate size. This step was necessary only occasionally since much of the computation involved the determination of a new optimum after a single aircraft or control parameter was changed. Next the search algorithm for minimizing the performance index (fig. 1) was used to adjust the same set of

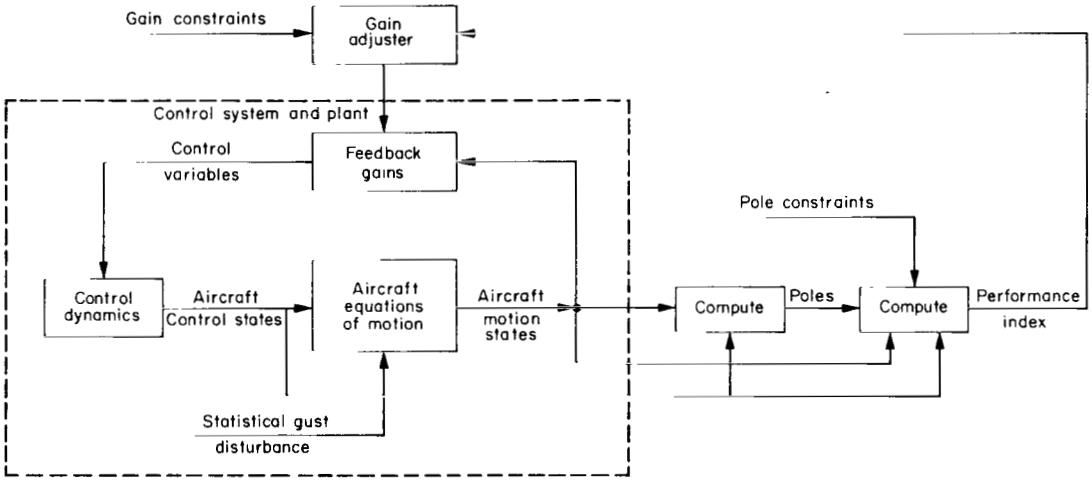

Figure 1.– Procedure for linear control system synthesis.

primary gains. The search algorithm was continued until changes resulting from successive iterations were sufficiently small that a value approaching the minimum was obtained. Finally, a search with all gains was made to reduce further the performance index to a value sufficiently close to the minimum. While the search algorithm used only ensures that a local minimum of the performance index is achieved, preliminary calculations are believed sufficient to reduce each search region to one with only a single local minimum.

In summary, the method developed provides a means for obtaining quantitative comparisons of the effects on control performance of changes in aircraft and control system parameters. In these comparisons, the control effort is restricted consistently by the selected constraints so that effects of parameter changes on performance are apparent. The addition of these constraints requires a more formidable computational procedure than would otherwise be required. Moreover, selections of the cost function coefficients and constraint parameters for the control criterion must be made realistically and some exploratory calculations may be required to determine suitable values.

APPLICATION OF THE METHOD TO AIRCRAFT CONTROL DURING LANDING APPROACHES

The method is applied to the control of two transport aircraft during the landing approach. The feedback gains required to minimize the performance index and the resulting minimum value of the index are determined as a function of nominal aircraft approach velocity for a subsonic aircraft and of aerodynamic control surface characteristics for a supersonic aircraft. The results are expressed as deviations of the aircraft and its controls from nominal conditions along the glide slope. In this section, the selection of the parameters needed to implement the synthesis procedure will be discussed.

Applicability of Method to Landing Approaches

Since the analysis is based on the determination of steady-state statistical averages, some discussion on the application of the method to finite length landing approach trajectories is needed. A transport aircraft nominal landing approach trajectory consists of a constant glide slope – constant velocity approach phase, and a flare phase during which the aircraft sink rate is reduced for touchdown. Only the approach phase is discussed here. The flight-path errors must be reduced sufficiently during the latter portion of this phase to ensure a satisfactory final touchdown.

An evaluation of the controlled aircraft response during the latter portion of the approach phase just prior to flare is the particular objective of this analysis. In order to ensure that effects of initial conditions at the beginning of the approach subside during the latter portion, a constraint is used on the damping of the real part of the closed-loop poles (first part of eqs. (6)). A constraint on the damping constant of $-0.04\ \text{sec}^{-1}$ was selected, since a typical time interval for the constant glide-slope phase of the landing approach is 1-1/2 min. Two other factors must be considered for the applicability of the steady-state analysis: (1) The gust representation, which will be described by linear stationary statistics, may actually vary as a function of altitude for the approach range of interest (100-1200 ft); and (2) if an angular altitude signal, such as an ILS glide-slope measurement, is used for altitude error information, either the effective altitude gain signal will vary with distance from the transmitter or horizontal distance corrections must be made to the glide-slope measurement. However, so long as these changes occur relatively slowly compared with the principal dynamics of the controlled aircraft, a computation based on steady-state statistics will be sufficiently accurate. A consequence of using these assumptions is that ensemble averages of aircraft motions will reach steady-state values at the final portion of the landing approach just prior to the landing flare phase. Hence, time-averaged stationary statistics can be used to represent the ensemble averages of motions during this final portion of the approach.

Equations of Motion

The synthesis procedure is applied to the control of longitudinal motions of the aircraft during landing approaches. The procedure provides a quantitative measurement of the ability to control the aircraft in the presence of specified horizontal and vertical gust disturbances with elevator and throttle controls. The equations of motion used for the analysis are given in appendix A. In these equations, five state variables (u, θ, $\dot{\theta}$, w, h) are used to describe deviations of the aircraft about the nominal flight path. With the assumption of first-order elevator and throttle dynamics, two additional state variables δ_e and δ_t which represent aircraft control positions, are obtained. The two control variables are designated u_{δ_e} and u_{δ_t}. The two gust disturbance variables u_g and w_g along with two barometric measured variables $u - u_g$ and $w - w_g$ complete the list of variables represented by the equations of motion (eq. (3)). For a constant nominal forward velocity, the $w - w_g$ variable is proportional to angle of attack within the accuracy of the linearized equations of motion; hence, it represents an angle-of-attack measurement. The effects of both inertial and barometric vertical velocity measurements are included in the results, but only a barometric horizontal velocity feedback is used. The previous equations consist of state variables describing aircraft and control motions. Additional state variable equations representing prescribed forms of filtering could also be added and appropriate constraints included for the filter parameters. For present examples, however, only feedback for selected aircraft equation-of-motion variables will be used for control.

In addition to a determination of the response of the system to random gust disturbances, a more complete analysis of control system requirements would include effects of wind shear disturbances and bias errors in the measured and control variables. For the control of these additional effects, feedback signals of integrals of the previously listed state variables (principally u and h) need to be added. For the present purpose of comparing effects of changes in aircraft parameters, these additional factors were neglected.

Gust Disturbance

The random gust disturbance used for the calculations is described in appendix C. Two forms of power spectra have been used to represent stationary turbulence (ref. 8). The first representation, the Dryden form, is a power spectrum expressed as a rational function of the frequency variable. The second, the Von Kármán form, is an irrational function of the frequency variable. The Dryden form can be used more readily for aircraft response calculation and has been more extensively used in analysis. The Von Kármán form has a somewhat firmer theoretical basis, and aircraft flight measurements tend to be in better agreement with this form. In appendix C, a fairly general comparison is made of the effects of these two forms of turbulence representation on elements of the system response covariance matrix used in the performance index evaluation. The comparison is expressed as a function of a gust frequency to system-pole frequency ratio, and the differences are relatively small when averaged over the frequency ratio range of interest. Hence, the simpler Dryden form (eqs. (C7) and (C8)) is used in the calculations in the body of the report. Gust scale lengths of 400 ft for the vertical gusts and 600 ft for the longitudinal gusts were selected. The relative rms magnitude used for the two gust components was $\sigma_{u_g}/\sigma_{w_g} = \sqrt{3/2}$. These gust parameters correspond approximately to typical values for the altitude range of interest reported in reference 9. The subsequent calculations are normalized to a unit value of σ_{w_g}.

Performance Index Coefficients

The factors considered for the selection of coefficients for the performance index are discussed in this section. The coefficients were selected with the objective of controlling altitude as accurately as possible while still maintaining reasonable values of the other variables. Altitude control is emphasized because it is indicative of horizontal touchdown dispersion, which is a primary task for the landing approach. Small altitude errors are desired particularly for an automatic landing system in which, at the initiation of the flare maneuver, altitude information is switched from an ILS glide slope to a radar altimeter. An altitude error signal relative to the glide slope results in a horizontal error in the initiation of the flare maneuver. The horizontal error resulting from the vertical error is a function of the cotangent of the nominal glide-slope angle. In the absence of any further horizontal distance information for the automatic landing system, this initial horizontal error cannot be corrected; hence a longitudinal touchdown error can occur. Furthermore, the ability to control altitude errors during the approach phase in the presence of disturbances is a principal measure of the ability to maintain flight-path control and hence to control horizontal dispersion at touchdown. The performance index coefficients were normalized with respect to altitude. Values of weighting coefficients for several other state variables were selected on the basis of the amount of error that could be tolerated relative to a reasonable value for altitude error. The range over which a variable could change without resulting in control limiting was also a consideration. The additional variables for which weighting coefficients are included are u^2, $\delta_e{}^2$, $\delta_t{}^2$, and $(w - w_g)^2$, which is proportional to angle of attack. The values used for the two aircraft are shown in tables 1 and 2. The inertial quantity u^2 provides a measure of horizontal velocity errors from a nominal steady-state value. The inertial horizontal velocity increment was used instead of the barometric since it was considered more important to maintain a desired average forward velocity than an instantaneous airspeed. The quantities $\delta_e{}^2$ and $\delta_t{}^2$, although actually state variables, were believed good indications of aircraft control motions, since the values of control dynamics were fixed. The $(w - w_g)^2$ coefficient depends on proximity to the stall angle and provides a weighting of angle-of-attack errors that becomes more important for nominal approach velocities close to the stall velocity. Generally, preliminary calculations were required to adjust some of the weighting function coefficients to values resulting in desired relative contributions of the states to the performance index. However, the presence of the constraints simplifies the selection process of the performance index coefficients from that required for the linear design case.

Constraints on Feedback Gains and Closed-Loop Poles

The selection of the gain and pole constraints (tables 1 and 2) is described in this section.

No feedback signals from the control states δ_e and δ_t were used, because the control dynamics were considered invariant quantities. Because of preliminary results, two feedback gains for the equation-of-motion states were also omitted. The $k_{\delta_e u}$ gain was omitted because, with the performance index weighted primarily for altitude control, the gain values that improved the performance index (primarily altitude errors) resulted in a deterioration of forward velocity control. The $k_{\delta_t \dot{\theta}}$ term was omitted because of its very small effect. In addition, the $k_{\delta_t u}$ feedback gain was omitted since only barometric horizontal velocity measurements were assumed. Ten adjustable feedback gains remained. Their limits were based on considerations of control saturation and measurement noise in the real system as previously described.

In the search procedure, the number of trial cases required depended on the number of gains to be adjusted and their initial proximity to final values. For the examples investigated, a preliminary search procedure resulted in at least one gain $k_{\delta_e\theta}$ always set at its constrained value. Hence, it was necessary to determine the values for a maximum of nine gains through use of the search procedure.

For the pole constraints, a damping ratio of at least 0.6 was selected to obtain fairly well damped transient behavior for the system. As previously described, a constraint on the real part of the poles of at least -0.04 sec^{-1} was used to ensure that steady-state conditions would be reached within the last portion of the final approach. The gain and pole constraints selected were sufficiently compatible that both sets of constraints were met for all cases calculated.

Comparison of Control Parameters for Subsonic and Supersonic Transports

To provide a meaningful comparison of the control performance of the two aircraft, some differences were introduced between the coefficients of the aircraft control states in the performance index δ_t^2 and δ_e^2 and the control gain constraints for each aircraft (tables 1 and 2). Since the larger supersonic aircraft has higher thrust engines, the limits (which are in dimensional form) for the throttle gains are larger by a factor of 3; in addition, since the allowable thrust excursions are greater for the supersonic transport, the weighting factor in the performance index is smaller. The aerodynamic control parameters were adjusted so that a steady-state control signal to the elevator would generate the same relative amount of aerodynamic control force for each aircraft. The parameter used to specify this relative amount is the ratio of elevator-control lift to total aircraft lift, $C_{L_{\delta_e}}/C_{L_\alpha}$. Since this ratio is approximately 50 percent larger for the subsonic transport than for the supersonic transport, the elevator gain limits for the supersonic transport are greater by 50 percent and the elevator weighting factor is smaller to compensate for the difference in relative control force.

The constraints on closed-loop poles are the same for both aircraft. Since the damping ratio pole constraint is a dimensionless form of degree of stability constraint, it is applicable over the range of frequencies of interest for both aircraft. The constraint on the real part of the poles $\Re_{\ell im}$ is the same since it requires that steady-state conditions be achieved within the same final approach time interval.

RESULTS AND DISCUSSION

The effects of several aircraft parameters on the ability of an automatically controlled aircraft to follow a nominal landing approach flight path in the presence of gust disturbances were compared. The performances of typical subsonic and supersonic transport aircraft were chosen as examples to demonstrate the technique. Control of only longitudinal motions was investigated. As an aircraft parameter was varied, the performance criterion was used to establish the best new set of control system gains for both elevator and throttle controls, and the corresponding system performance was determined. The aircraft parameters varied were approach velocity for the subsonic aircraft and control surface location for the supersonic aircraft. The results provide quantitative comparisons of linear closed-loop control performance for various nominal conditions.

The nominal flight path used was a 3° glide slope with a constant approach speed. The results presented are based on statistical averages (variances) of deviations of aircraft motions from nominal values for the latter portion of the approach flight path. Effects of both vertical and horizontal gust disturbances are included.

Subsonic Transport Performance

The parameters used to represent a swept-wing subsonic jet transport are shown in table 1; the control system parameters, performance index coefficients, and pole and gain constraints are also shown. Performance index coefficients were selected to emphasize control of altitude errors. Some additional description of the selection of the control parameters was given in the previous section.

Effect of variations in approach velocity– The performance criterion was used to determine the control system parameters and resulting control performance for a range of nominal approach velocities. The performance index (eq. (4)) and the statistical averages (variances) of several variables included in the performance index are shown in figures 2 through 6. These averages are indicative of conditions for the latter portion of the landing approach. While the velocity range shown is larger than that normally considered for a landing approach, it is useful for illustrating trends. An example of control parameter variations is provided by different restrictions on the vertical feedback signals. The three feedback signals were as follows: The inertial vertical velocity system represents the case in which the five state variables in the open-loop equations of motion, including inertially measured vertical velocity, are fed back, but barometric vertical velocity is not included. The no-vertical-velocity case includes the same set of feedback variables except that both vertical velocity feedbacks are omitted from the elevator and throttle control signals. The barometric vertical velocity case represents the use of angle-of-attack feedback in place of the inertial vertical velocity signal. The same gain constraint and performance index coefficients were used for both vertical velocity feedback quantities. For the longitudinal velocity measurement, only barometric feedback was used.

The variations with approach velocity shown in figure 2 indicate that errors, as determined by the performance criterion, become larger for the slower approach speeds. The error in altitude control with approach velocity is shown in figure 3. For example, it can be seen that the errors are three times larger at 110 knots than at 150 knots for the vertical velocity feedback case. Also, a comparison of figures 2 and 3 indicates that altitude error is a principal component of the performance index for the barometric and vertical velocity cases, although its contribution is less for the inertial vertical velocity case. This comparison can be made directly since the performance index was normalized with respect to altitude.

Three effects were found to contribute to the deterioration in performance at the slower velocities. The first effect is that constant magnitude gust disturbances tend to produce larger aerodynamic disturbing forces relative to the aerodynamic control forces for the slower approach velocities. The vertical velocity disturbances result in larger angle-of-attack disturbances, and the horizontal velocity disturbances are relatively larger at the decreased approach velocities. The second effect is that the drag variation with angle of attack at low velocities becomes more unfavorable. For approach speeds less than about 135 knots, the drag variation with angle of attack C_{D_α} is large enough that the variation of drag with steady-state velocity (at constant lift) is negative. Although not shown separately, the deterioration in altitude performance is quite

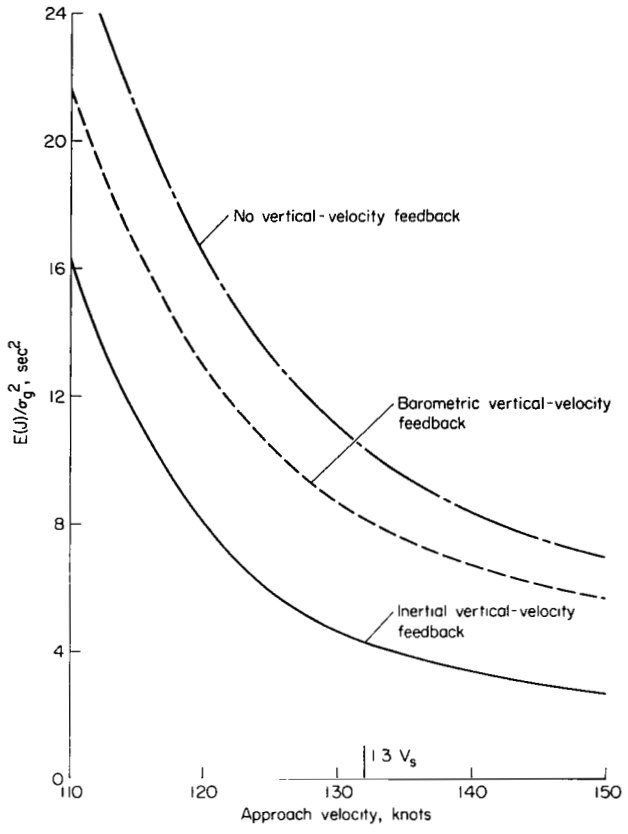

Figure 2.– Effect of approach velocity on control performance for subsonic transport.

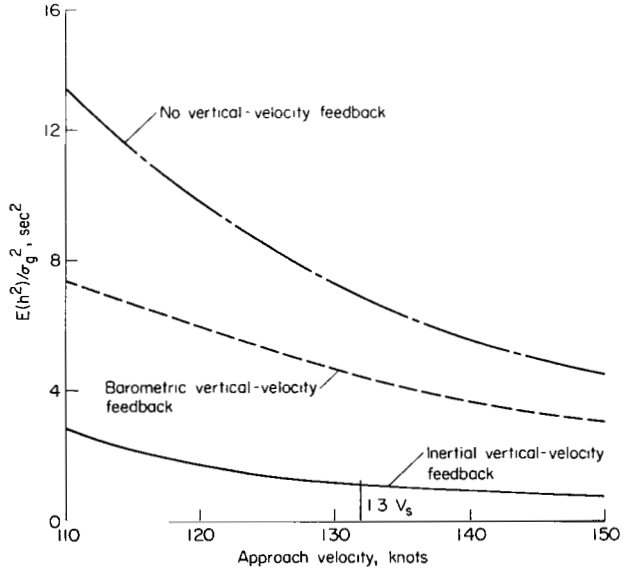

Figure 3.– Effect of approach velocity on altitude errors for subsonic transport.

dependent on values of the derivative C_{D_α} for the lower velocities. This deterioration occurs in both forward velocity and altitude control. The third effect is that an increased weighting of barometric vertical velocity used for the slower approach velocities results in greater adjustments in system gains to reduce angle-of-attack errors. This increased weighting of vertical velocity tends to increase the performance index. Even though the vertical velocity is decreased somewhat, the reduced emphasis on the control of other quantities in the performance index such as altitude results in greater errors for these quantities and in corresponding increases in the performance index.

The variation with nominal approach velocity of two other elements of the performance index, vertical velocity and elevator control, is shown in figures 4 and 5. Vertical velocity errors (fig. 4) are less sensitive to variations in approach velocity than are altitude errors (fig. 3). The deterioration in altitude performance with slower approach velocity occurs even with an increase in elevator control effort (fig. 5). Although not shown, the forward velocity errors were not significantly larger in the slower velocity range as long as control was determined through simultaneous use of the elevator and throttle.

With regard to relative effectiveness of the vertical velocity signals, the use of the inertial signal resulted in the best performance of the three feedback configurations; this was to be expected, since control to a fixed flight path was desired. The usefulness of the inertial vertical velocity signal is shown by the deterioration in performance when this feedback quantity was omitted. That is, for a nominal approach velocity of 1.3 times the stall velocity, the performance for the no-vertical-velocity feedback case is worse by a factor of 3 than that of the inertial vertical velocity case (fig. 2). Substitution of

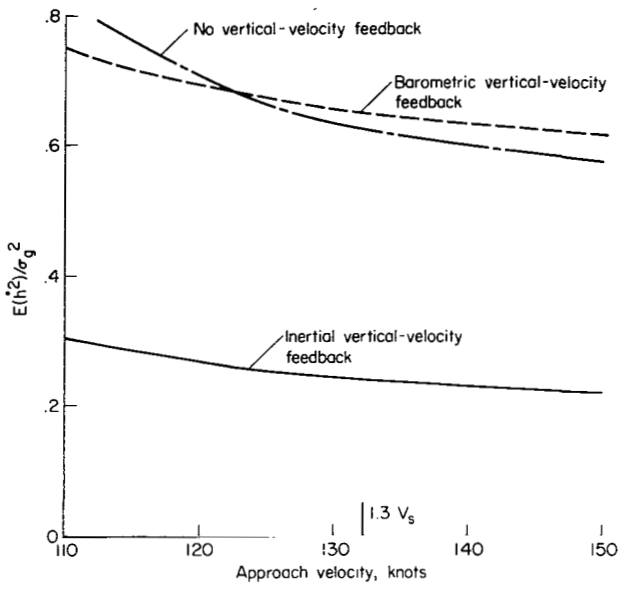

Figure 4.– Effect of approach velocity on altitude rate errors for subsonic transport.

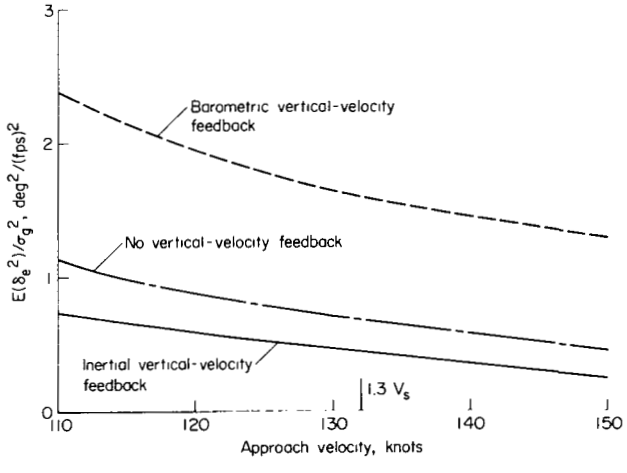

Figure 5.– Effect of approach velocity on elevator motion for subsonic transport.

barometric vertical velocity feedback for inertial vertical velocity feedback results in intermediate performance between the other two cases, since interfering effects of the gust disturbances are present in this signal. The feedback changes shown are intended primarily as examples of the method; other types of changes in the feedback signals, such as blending and filtering of the signals, were not investigated.

Effects of approach velocity changes on vertical velocity errors and elevator motion are shown in figures 4 and 5. The elimination of the inertial velocity feedback increased the vertical velocity variance by a factor of 3 (fig. 4). This deterioration was similar to the change in altitude error (fig. 3). However, the addition of barometric feedback did not result in any appreciable improvement in vertical velocity errors as was the case for altitude errors. The use of barometric vertical velocity feedback resulted in a considerably greater amount of elevator motion than did either of the other two cases (fig. 5). However, the amount of elevator motion in any case was quite small. Although not shown, a reduction in the elevator weighting factor in the performance index did not cause any significant change in the components of the performance index. Hence, the small magnitude of the elevator motion is attributed primarily to the constraints.

The computed results depend directly on the particular gain and pole constraints that actually restrict the set of gains that minimizes the performance index. One gain $k_{\delta_e\theta}$ was always at its constrained value. The results are therefore quite dependent on the value selected for this constraint. The damping ratio constraint generally resulted in a gain constraint boundary due to one or two pairs of closed-loop poles, and also resulted in a significant effect on the performance index. However, the restriction on the real part of the poles had only a small effect on the final sets of gains and a corresponding minor effect on final values of the performance index.

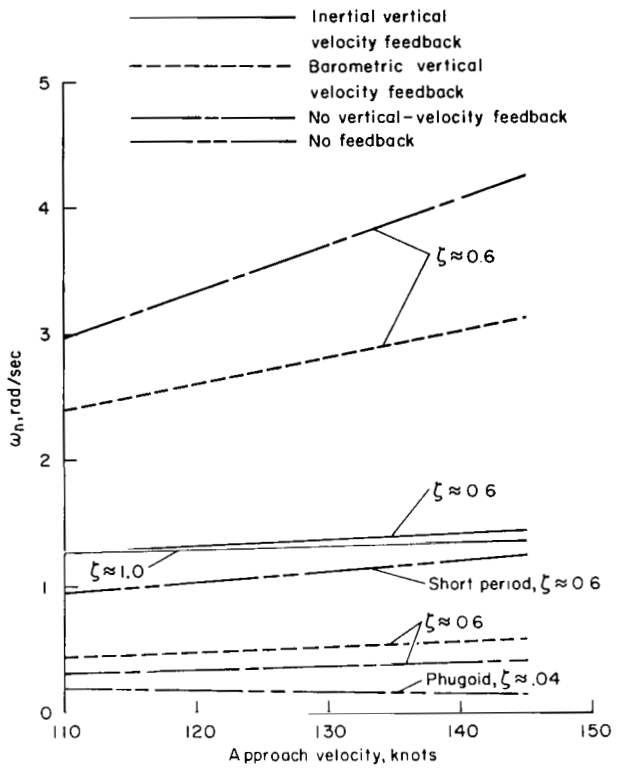

Figure 6.-- Effect of approach velocity on aircraft natural frequencies for subsonic transport.

The closed-loop pole patterns depend on the feedback configuration used and generally consist of three real and two complex pairs of poles for the closed-loop systems investigated. The three real poles are related to the two control dynamics modes and an equation-of-motion mode whose components are predominantly altitude and forward velocity. The two oscillatory modes are related to the short-period and phugoid aircraft modes. Variations in ω_n for these two modes for the three optimized feedback configurations are shown in figure 6. The open-loop short-period and phugoid mode frequencies are also shown, and the average damping ratio for the velocity range computed is indicated for each mode. For the barometric and no-vertical-velocity feedback cases, the set of gains for best performance results in two complex pairs with the damping ratio near the stability constraint value of $\zeta = 0.6$. For the inertial velocity feedback case, only one complex pair is near the stability constraint boundary, and the other is near the real axis. In general, while a preliminary adjustment of gains to achieve an approximate pole pattern was desirable, this adjustment could not be relied on entirely to obtain the best performance.

The gust disturbance frequencies were compared with the controlled aircraft frequencies. For the gust scale lengths previously selected and an aircraft velocity of 130 knots, the frequencies of the pole locations for the vertical and horizontal gusts are 0.55 and 0.37 rad/sec, respectively. A comparison with figure 6 shows that the gust disturbance frequencies are within the controlled aircraft frequency range, with the result that the gusts provide a greater excitation to the lower frequency modes.

In this investigation, changes due to the aerodynamic surface control were emphasized. The contributions of the throttle control and forward velocity to the performance index, which is weighted primarily for altitude control, remained fairly constant for the range of parameters varied except for the slowest approach velocities. Although the use of the throttle was essential to maintain forward velocity control, throttle gains beyond the level necessary to minimize the performance index did not significantly decrease altitude errors. Although not specifically shown, an alternate coupling effect tended to prevail: larger elevator gains tended to reduce forward velocity errors.

Performance for nominal approach velocity– A more complete description of the results obtained for the 132-knot approach velocity (1.3 V_S) is shown in table 3. (The FAA generally specifies a velocity 30 percent higher than stall as a minimum desired approach speed for transport aircraft.) The table shows the variances of all state variables as well as the control system gains. Note that although all state variables were not included in the performance index, they were controlled to within reasonably small values. Further, only the $k_{\delta_e \theta}$ gain is at the constraint value, while the other gains have been adjusted to minimize the performance index. It should be mentioned that some redundancy was present in the selection of several throttle gains so that nearly the same minimum performance index could be achieved by somewhat different combinations of the gains.

Table 3 also shows the maximum rms of the random gusts that can be controlled by each system to the accuracies recommended by the FAA for Category II (100–ft decision height, ref. 10). Only the vertical gust magnitude is shown, since a constant ratio of vertical to horizontal gust magnitudes, normalized to a unit vertical gust, has been used in the calculations. The FAA accuracy requirements are ±12-ft altitude and ±5-knot forward speed. If it is assumed that the accuracy requirements are based on a 5-percent probability of being exceeded and that the errors have a gaussian probability density distribution, then the tolerance for altitude error is 6-ft rms (36-ft^2 variance), and the velocity error tolerance is 8.4 fps (71 fps^2 variance). An inspection of the altitude and forward speed variances in table 4 indicates that altitude is the most critical quantity. The maximum gust disturbances for which the systems can still achieve the altitude tolerance are shown in the table. An indication of the cumulative probability of these gust disturbances occurring is given in reference 9. For instance, at an altitude of 250 ft, the probability of exceeding a 4-fps rms vertical gust region is approximately 15 percent. The results in table 4 indicate that with the constraints selected for this example, an inertial vertical velocity signal should be included to achieve adequate control of this magnitude of turbulence. Note that this example could have been extended to determine the overall probability of exceeding the altitude tolerance for all levels of turbulence. The probability would be determined by an integration using a probability density distribution of rms levels of turbulence, which could be obtained from a cumulative probability curve such as that given in reference 9. However, calculations made of system errors based on particular turbulence levels are also felt to be directly useful, since, in operational use, local meteorological conditions could be measured to establish existing rms gust levels.

Supersonic Transport Performance

Several calculations were made for an example supersonic transport with variable-sweep wings fixed in the forward position. Characteristics of the aircraft and the control parameters were listed in table 2. Differences between the subsonic and supersonic aircraft necessitated some differences in the selection of gain constraints and cost function coefficients and these changes are described in a previous section. Although selection of these constraints and coefficients was necessarily somewhat qualitative, it is believed that the result is a reasonable comparison of the control performance of the two aircraft. Only performance index coefficients for the aircraft control variables δ_e and δ_t were changed to account for differences in elevator and throttle effectiveness between the two aircraft.

Basic supersonic transport performance and comparison with subsonic transport– The control performance for the supersonic transport at a nominal approach velocity of 145 knots is compared for several forms of vertical velocity feedback (table 4). Results for the subsonic transport at the

same approach velocity are also included in the table. Effects of changes in the vertical velocity feedback are similar for the two aircraft. However, the performance of the supersonic transport is worse than that of the subsonic transport for all feedback combinations, although the difference varies considerably with each combination. For instance, the ratio of the performance indices for the two aircraft varies from a factor of 2.6 for the inertial velocity feedback case to a ratio of 1.3 for the no-vertical-velocity feedback case.

At least two factors contribute to the poorer performance of the supersonic aircraft. One factor is that the altitude-changing capability of elevator-controlled aircraft depends largely on the ability to rotate the aircraft to generate a change in angle of attack and hence to produce a vertical acceleration. An indication of the relative available pitching angular acceleration for the two aircraft is the open-loop pitching acceleration per unit elevator angle deflection. The value of this quantity for the supersonic transport is only about 10 percent of that for the subsonic transport at the same dynamic pressure. Even though elevator gain constraints were increased by a factor of 50 percent for the supersonic transport, the average applied angular acceleration can be expected to be much less for the supersonic transport. The other factor is the amount of vertical acceleration disturbance produced by a vertical gust, and it depends on the ratio of dimensional lift-curve slope to aircraft mass, which is approximately the same for the two aircraft. The value for the larger transport is higher than would normally be expected, and is partly a consequence of the small amount of wing sweep in the landing configuration, which results in a fairly high lift-curve slope. Hence, vertical gusts cause approximately the same amount of vertical acceleration disturbance for the supersonic transport as for the subsonic transport, but the control effectiveness to counteract these disturbances is appreciably less. This trend toward reduced control effectiveness is fairly typical for larger aircraft.

Variations in gust disturbance– The separate effects of horizontal and vertical gust components and of variations in gust scale length are compared in table 5. The set of gains used for these comparisons was obtained by the optimization procedure based on the vertical plus horizontal gusts used in previous calculations. The separate effects of the vertical and horizontal gust disturbances are shown in the first two rows. The influence of reducing the gust scale length for both the vertical and horizontal gusts is shown in the next two rows of table 5. The reduced scale length results in a decrease in the effect of the disturbance for both cases, and thus the selection of this parameter has a significant effect on the results. Note that both the increased magnitude and the increased gust scale length for the horizontal gust tend to increase the effect of the horizontal disturbance relative to the vertical gust. However, the vertical gust is still seen to have the major effect. Another example of effects of a change in the gust parameters is given subsequently.

For a final comparison, results for a vertical gust with a horizontal spectral form (eq. (C7)) are shown. In this comparison, the horizontal form scale length is two-thirds of, and the variance is the same as, that used previously for the vertical gust. This form of comparison of the horizontal and vertical gust spectra results in matching the high-frequency portions of the two spectra. The comparison of the effects of the two spectral forms of the vertical gusts (first and last rows of table 5) indicates that the differences in lower frequency content have a moderate effect on the magnitude of the controlled aircraft response. Note that values of the performance index and altitude are changed by different fractional amounts by the horizontal spectral form of disturbance. Although not shown, other state variables were changed by different relative amounts; therefore, results for the two disturbances could not be made identical by a suitable choice of gust scale length and variance of the horizontal form of disturbance.

Variations in aerodynamic control effectiveness– As a further illustration of the utility of the performance criterion, effects of varying the aerodynamic control effectiveness were investigated. Values of lift and moment effectiveness C_{L_δ} and C_{m_δ} were varied (figs. 7 and 8), while the cost function coefficients and pole and gain constraints given in table 2 were held constant. This type of variation provides a means of evaluating the relative effectiveness of the lift and moment control contributions. While the relatively large variations shown may not be feasible to implement, they permit a more clear illustration of trends. These variations can be interpreted as representing the relative performances of aerodynamic control surfaces with different sizes and longitudinal locations. Another interpretation is that the variations represent two different control surfaces driven by a common signal to achieve a particular combination of lift and moment effectiveness. While better performance for two control surfaces would be obtained, in general, through the use of separate control signals to drive each surface, the objective here is to investigate the influence of a single aerodynamic control effectiveness term. Changes in lift coefficient effectiveness (fig. 7) could be obtained, for instance, through the addition of an approximately pure lift control connected linearly to the elevator control. For negative values of C_{L_δ}, sufficient lift has been added to counteract the elevator lift that both lift and moment effectiveness terms tend to change altitude in a common direction. The performance is seen to improve with more negative C_{L_δ}. For instance for the inertial vertical velocity feedback case, the performance index varies from a value of 9.5 to 4.8. Despite the relatively large lift coefficient variation shown, the performance index changes only a moderate amount. Hence, the moment effectiveness is seen to predominate for the fairly low frequency range that has been excited by the gust disturbance. A comparison of the performance index and altitude curves indicates that altitude is the major portion of the performance index.

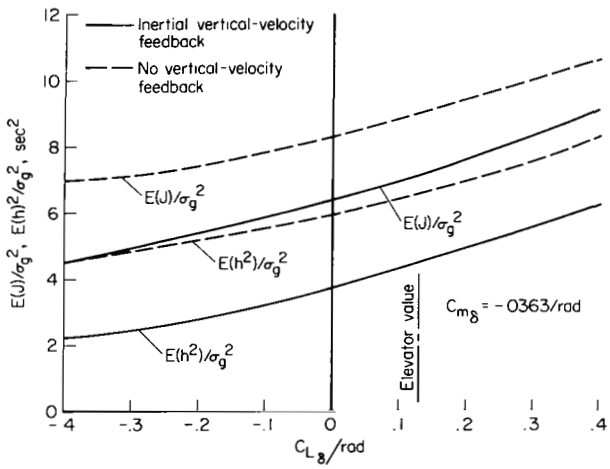

Figure 7.– Effect of variations in lift effectiveness on control performance for supersonic transport.

Results for changes in pitching-moment effectiveness (with constant lift effectiveness) are shown in figure 8. A value of lift coefficient considerably greater than that for the elevator was selected to better show tradeoff characteristics with the moment coefficient variations. Hence, a relatively large control surface is represented. In figure 8(a), the previous values of scale length and magnitude for the vertical and horizontal gust velocities are used, while in figure 8(b), the values used for both components are $L_u = L_w = 300$ ft, $\sigma_{u_g} = \sigma_{w_g} = 1$ fps. A rather large range of C_{m_δ} is shown; this range includes values that cause altitude changes in the same as well as the opposite direction from that due to C_{L_δ}. These variations could represent different longitudinal locations of control surfaces that effectively act either forward (canard surface) or aft (conventional elevator) of the aircraft center of gravity. The higher positive values shown for moment effectiveness result in the best values of the performance index J, since the moment and lift effectiveness act together in the control of altitude. For the range of positive moment effectiveness shown, performance is not improved much beyond that obtained through use of lift control alone ($C_{m_\delta} = 0$). On the other hand, values of negative moment (the direction that tends to oppose the lift effect) result in a

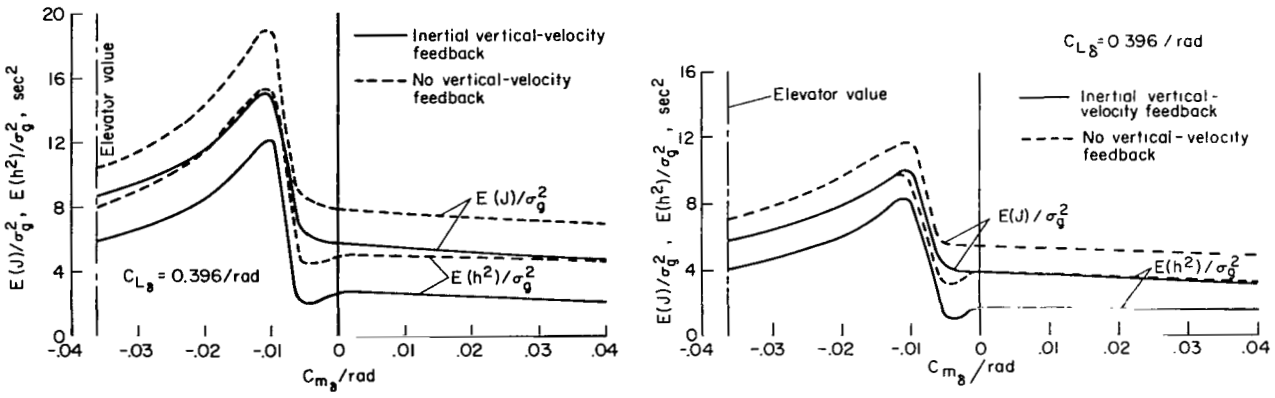

(a) Gust parameters, L_u = 600 ft, L_w = 400 ft, $\sigma_{u_g} = \sqrt{3/2}$ fps, σ_{w_g} = 1 fps

(b) Gust parameters, $L_u = L_w$ = 300 ft, $\sigma_{u_g} = \sigma_{w_g}$ = 1 fps

Figure 8.– Effect of variations in moment effectiveness on control performance for supersonic transport.

considerable deterioration of performance. The maximum deterioration occurs for a value of the control surface center of pressure $C_{m_\delta}/C_{L_\delta}$ that is somewhat more negative than the value of the disturbance center of pressure $C_{m_\alpha}/C_{L_\alpha} = -0.0137$. The latter ratio is indicative of the longitudinal center of pressure for the vertical gust disturbance, since this disturbance is assumed to produce an angle-of-attack change. The relative values of the two ratios can be obtained from figure 8 by a comparison of the C_{m_δ} values with the value of $C_{m_\alpha}C_{L_\delta}/C_{L_\alpha} = -0.0054$. For negative values of moment that have a smaller magnitude than 0.0054, there is only a relatively small deterioration in performance. In fact, the altitude variance improves slightly in this range. The principal reason for this difference in trends between the performance index and altitude is a sharp increase in control motion, which nevertheless makes only a small contribution to the performance index. As the moment effectiveness becomes more negative, the performance deteriorates sharply. The poorest performance occurs for a value of pitching moment that results in a control center of pressure about 2.5 percent aft of the center of gravity. While the center-of-pressure location of typical wing flaps generally would be farther aft of this value, the location for certain types of spoilers may be close to it. Although not shown, a reversal of the aerodynamic control surface gains occurs in the region of poor performance. The reversal of the various gains occurs over a narrow range of C_{m_δ} in which performance is poorest (fig. 8) rather than at a particular value. A sufficient degree of controllability is always available, however, to meet the pole region constraint within the gain limits selected. Although not separately shown, the forward velocity errors showed a similar deterioration with slightly negative values of moment effectiveness, but these changes were less extreme than the changes in altitude errors.

Figure 8(b) shows the effect on moment effectiveness variations of a reduction in the gust scale length for the horizontal and vertical gusts and a reduction in the magnitude of the horizontal gust length from that used in figure 8(a). A comparison of figures 8(a) and 8(b) indicates that values of the performance index and altitude are quite sensitive to these changes. In addition to the expected effect of the reduction in horizontal gust magnitude, the reduction in the gust scale lengths (increase in disturbance frequency) also leads to an improvement in the ability to control the disturbance. This improvement is a consequence of a reduction in the low-frequency excitation on which altitude control depends. However, the performance curve shape is seen to be quite similar

to the previous one (fig. 8), so that in a comparative sense the trend due to the aerodynamic parameter C_{m_δ} is still the same. Although not shown, the set of gains for each value of C_{m_δ} was essentially the same for the two cases.

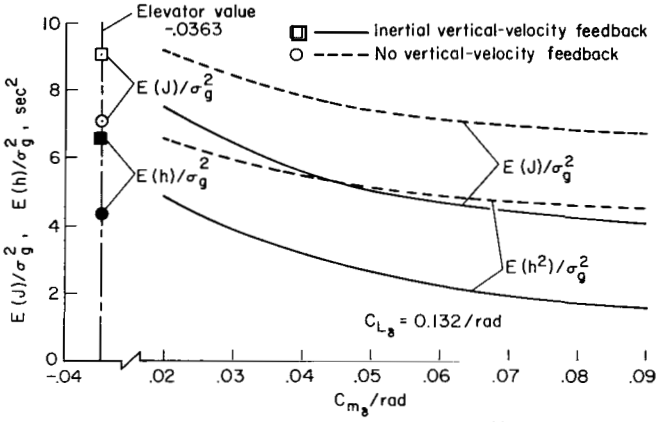

Figure 9.– Effect of variations in moment effectiveness of canard control of performance for supersonic transport.

Other effects of control changes are shown in figure 9. The variation in moment effectiveness, with control lift acting to correct altitude in the same direction as the moment, is an example of what could be achieved with canard surfaces at different longitudinal locations that have the same lift effectiveness as the elevator control. Note that this value of C_{L_δ} is smaller than that used in figure 8. Values of elevator performance are indicated by the points at $C_{m_{\delta_e}} = -0.0363$. The maximum value of moment effectiveness shown, about three times the value of the elevator moment effectiveness in the basic configuration, is seen to result in somewhat better performance than the best value from figure 8(a), in which a larger value of lift effectiveness was used.

CONCLUSIONS

A technique has been developed for minimizing a performance index in the presence of constraints to give a quantitative evaluation of the ability of an automatically controlled aircraft to follow a preselected landing approach path in the presence of gust disturbances. The technique has been applied to a subsonic and a supersonic jet transport, using representative performance index and constraint parameters. The utility of this type of criterion is illustrated by evaluating changes in control performance due to changes in some of the longitudinal aircraft and control parameters. The variations in control performance were, for the most part, in directions that would be expected intuitively. However, the intent was to provide a means for quantitatively evaluating these changes.

The principal results are summarized as follows:

1. Slower nominal approach velocities resulted in considerable deterioration in control performance for a typical subsonic transport.

2. The use of an inertial vertical velocity feedback signal was found to be more effective than a barometric velocity (angle of attack) signal for improving performance in the presence of gust disturbances.

3. The control performance of a smaller subsonic transport was superior to that of a large supersonic transport configuration.

4. Effects of control surface longitudinal location on control performance for the supersonic transport were quite significant. Tradeoffs were determined for varying amounts of aerodynamic lift and moment effectiveness, and it was found that moment effectiveness predominated for most of the parameter ranges investigated. However, for one range that resulted in a control center of pressure slightly aft of the aircraft center of gravity, the performance deteriorated quite markedly.

5. A brief examination was made of possible interacting effects between the control and several state variables that normally might not be expected to be very large. The elevator control was found to have an effect on the reduction of forward velocity errors as well as the expected predominant effect on altitude errors.

6. The flight-path errors were shown to be fairly sensitive to the parameters selected for the gust disturbance.

Ames Research Center
National Aeronautics and Space Administration
Moffett Field, Calif., 94035, Sept. 14, 1970

APPENDIX A

EQUATIONS OF MOTION

The linearized equations for the aircraft motions and the control dynamics, together with the gust velocity disturbance equations, are given in this appendix. The longitudinal aircraft equations of motion are based on a summation of horizontal and vertical forces and of pitching moment, and are expressed in the stability axis system (ref. 11). This system is a body axis system that expresses deviations of the aircraft relative to a constant velocity vector. For the present case, this vector is along the approach glide slope. Terms representing the gust velocity disturbance must also be added to the terms describing motions of the aircraft given in reference 11. A one-dimensional representation of each component of gust velocity (ref. 12) is used, which neglects spanwise distributions of gust intensity. Effects of instantaneous spatial longitudinal distributions of gust velocities are also omitted. The aerodynamic forces due to translations are determined by the difference between the aircraft and instantaneous gust velocities. The resulting equations expressed in the stability axis system are as follows.

Drag equation:

$$\dot{u} + \frac{\rho U_o S C_{D_o}}{m} u - \frac{\rho U_o S}{2m} (C_{L_o} - C_{D_\alpha}) w + g\theta = X_{\delta_t}\delta_t + \frac{\rho U_o S C_{D_o}}{m} u_g - \frac{\rho U_o S}{2m} (C_{L_o} - C_{D_\alpha}) w_g \tag{A1}$$

Lift equation:

$$\dot{w} - U_o\dot{\theta} + \frac{\rho U_o S C_{L_o}}{m} u + \frac{\rho U_o S}{2m} (C_{L_\alpha} + C_{D_o}) w + \frac{C_{L_{\dot{\alpha}}} \rho S c}{4m} \dot{w} + \frac{C_{L_q} \rho U_o S c}{4m} \dot{\theta} = Z_{\delta_t}\delta_t - \frac{C_{L_{\delta_e}} \rho U_o^2 S}{2m} \delta_e + \frac{\rho U_o S C_{L_o}}{m} u_g + \frac{\rho U_o S}{2m} (C_{L_\alpha} + C_{D_o}) w_g \tag{A2}$$

Moment equation:

$$\ddot{\theta} - C_{m_o} \frac{\rho U_o Sc}{I_y} u - \frac{\rho U_o Sc}{2I_y} C_{m_\alpha} w - \frac{\rho Sc^2}{4I_y} C_{m_{\dot{\alpha}}} \dot{w} - \frac{\rho U_o Sc^2}{4I_y} C_{m_q} \dot{\theta}$$

$$= M_{\delta_t} \delta_t + \frac{\rho U_o{}^2 Sc}{2I_y} C_{m_{\delta_e}} \delta_e - C_{m_o} \frac{\rho U_o Sc}{I_y} u_g - C_{m_\alpha} \frac{\rho U_o Sc}{2I_y} w_g \tag{A3}$$

The linearized kinematic relation to obtain the vertical velocity perpendicular to the constant glide slope is:

$$\dot{h} = U_o \theta - w \tag{A4}$$

Equations (A1) through (A4) are used to determine motions that are incremental changes from the nominal constant glide slope – constant velocity approach path. A total of five state variables (u, θ, $\dot{\theta}$, w, h) are obtained for the description of the aircraft motions.

Noise-free measurements of these states are assumed available. For actual transport aircraft landing approaches, altitude errors would normally be obtained from ILS angle measurements; hence, to obtain a control signal equivalent to that of an altitude signal with constant gain, the gains to be used with an angular measurement would need to be continuously adjusted for horizontal distance changes. However, this variation occurs fairly slowly, and a determination of the amount of gain adjustment actually required is not included in the analysis.

The control dynamics are assumed to be expressible in linear first-order form; they represent principally elevator-servo dynamics for the elevator control and engine dynamics for the throttle control. The equations are (with unit gain used for convenience):

$$\dot{\delta}_e = - \frac{\delta_e}{\tau_e} + \frac{u_{\delta_e}}{\tau_e} \tag{A5}$$

$$\dot{\delta}_t = - \frac{\delta_\tau}{\tau_t} + \frac{u_{\delta_\tau}}{\tau_t} \tag{A6}$$

Equations (A1) through (A6) are combined into the following first-order matrix form to be used in the analysis:

$$\dot{\underline{x}} = A\underline{x} + B\underline{u}_c + C\underline{v} \tag{A7}$$

where

the $\underline{x}$ vector represents the seven state variables ($u, \theta, \dot{\theta}, w, h, \delta_e, \delta_t$)
the $\underline{u}_c$ vector represents the two control variables ($u_{\delta_e}, u_{\delta_t}$)
the $\underline{v}$ vector represents the two gust disturbance variables (u_g, w_g)

The elements of the A, B, and C matrices are as follows.

$$A = \begin{array}{c} \begin{matrix} \quad U & \quad \theta & \quad \dot{\theta} & \quad\quad w & \quad h & \quad \delta_e & \quad\quad \delta_t \end{matrix} \\ \begin{bmatrix} -C_{D_o}\frac{k_1}{m} & -g & 0 & (C_{L_o} - C_{D_\alpha})\frac{k_1}{2m} & 0 & 0 & X_{\delta_t} \\ 0 & 0 & 1 & 0 & 0 & 0 & 0 \\ (C_{m_o} - C_{L_o}k_4k_5)\frac{k_1 c}{I_y} & 0 & \left[C_{m_q} + (4m - C_{L_q}k_5)k_4\right]\frac{k_1 c^2}{4I_y} & \left[C_{m_\alpha} - k_4k_5(C_{L_\alpha} + C_{D_o})\right]\frac{k_1 c}{2I_y} & 0 & (C_{m_{\delta_e}} - C_{L_{\delta_e}}k_4k_5)\frac{k_3 c}{I_y} & M_{\delta_t} + \frac{k_4k_5mcZ_{\delta_t}}{I_y} \\ -4C_{L_o}k_1k_2 & 0 & (4m - C_{L_q}k_5)k_2U_o & -2cSk_2(C_{L_\alpha} + C_{D_o})U_o & 0 & -2C_{L_{\delta_e}}U_ok_1k_2 & 4mk_2Z_{\delta_t} \\ 0 & U_o & 0 & -1 & 0 & 0 & 0 \\ 0 & 0 & 0 & 0 & 0 & -\frac{1}{\tau_e} & 0 \\ 0 & 0 & 0 & 0 & 0 & 0 & -\frac{1}{\tau_t} \end{bmatrix} \end{array}$$

where

$$k_1 = \rho U_o S$$

$$k_2 = 1/(4m + C_{L_{\dot{\alpha}}}\rho Sc)$$

$$k_3 = (1/2)\rho U_o^2 S$$

$$k_4 = C_{m_{\dot{\alpha}}}/(4m + C_{L_{\dot{\alpha}}}\rho Sc)$$

$$k_5 = \rho Sc$$

$$B^t = \begin{array}{c} \begin{matrix} U & v & \dot{v} & w & h & \delta_e & \delta_t \end{matrix} \\ \begin{bmatrix} 0 & 0 & 0 & 0 & 0 & \frac{1}{\tau_e} & 0 \\ 0 & 0 & 0 & 0 & 0 & 0 & \frac{1}{\tau_t} \end{bmatrix} \end{array} \begin{matrix} \\ u_{\delta_e} \\ u_{\delta_t} \end{matrix}$$

$$C^t = \begin{array}{c} \begin{matrix} & & & & & & \end{matrix} \\ \begin{bmatrix} C_{D_o}\frac{k_1}{m} & 0 & (C_{L_o}k_4k_5 - C_{m_o})\frac{k_1 c}{I_y} & 4C_{L_o}k_1k_2 & 0 & 0 & 0 \\ (C_{D_\alpha} - C_{L_o})\frac{k_1}{2m} & 0 & \left[k_4k_5(C_{L_\alpha} + C_{D_o}) - C_{m_\alpha}\right]\frac{k_1 c}{2I_y} & 2c\,Sk_1(C_{L_\alpha} + C_{D_o})U_o & 0 & 0 & 0 \end{bmatrix} \end{array} \begin{matrix} \\ u_g \\ w_g \end{matrix}$$

The control signals are in the form of a linear combination of the measured quantities and can be expressed as follows:

$$\underline{u}_c = -K\underline{x} - K_V(\underline{x}_V - \underline{v}) \qquad \text{(A8)}$$

where $\underline{x}_V$ is the portion of the state vector that represents the two velocity variables u and w, and K_V is a 2X2 gain matrix that relates the gains from the two barometric velocity variables to the two control variables.

Two forms of feedback signals are indicated in equation (A8). The primary signals are from the inertially measured state variables, which indicate aircraft motions relative to a fixed reference frame. The other feedback signal shown, termed a "barometric measurement," is obtained from differences between aircraft velocities and gust disturbance velocities. The barometric vertical velocity component is an angle-of-attack ($\alpha = w/U_O$) type of measurement since the nominal approach velocity is a constant value. The horizontal velocity component represents an air speed type of measurement.

The equations of motion for the closed-loop system are obtained by substituting equation(A8) into equation (A7)

$$\dot{\underline{x}} = (A - BK)\underline{x} - BK_V(\underline{x}_V - \underline{v}) + C\underline{v} \tag{A9}$$

The method used to evaluate the performance index from these equations is given in appendix B.

APPENDIX B

EVALUATION OF THE PERFORMANCE INDEX

The equations used to calculate the performance index J from a preselected set of feedback control gains K and K_V are presented in this appendix. The performance index is determined from steady-state time averages of the response of the system to a stationary statistically described gust disturbance by a frequency domain method.

The first-order linear equations of motion of the system with linear feedback terms, expressed in equation (A9), are of the following time domain form

$$\dot{\underline{x}} = (A - BK)\underline{x} - BK_V(\underline{x}_V - \underline{v}) + C\underline{v} \tag{B1}$$

It is convenient to combine the matrices in equation (B1) into

$$\dot{\underline{x}} = (A - BK)\underline{x} - BK_V\underline{x}_V + (BK_V + C)\underline{v}$$

$$= D\underline{x} + C_V\underline{v} \tag{B2}$$

The D and C_V matrices can be constructed from the appropriate matrices in equation (B1) by the addition of corresponding elements (since the vector, $\underline{x}_V$, is contained in $\underline{x}$).

The performance index to be calculated from the equations of motion is given by:

$$J = E(\underline{x}^tQ\underline{x}) + E[(\underline{x}_V - \underline{v})^tP(\underline{x}_V - \underline{v})] \tag{B3}$$

where P and Q are symmetric matrices. For convenience in the analysis, equation (B3) is rearranged into the following form:

$$J = \text{trace}\left\{QE(\underline{x}\underline{x}^t)\right\} + \text{trace}\left\{P[E(\underline{x}_V\underline{x}_V^t) - 2E(\underline{v}\underline{x}_V^t) + E(\underline{v}\underline{v}^t)]\right\} \tag{B4}$$

The $E(\underline{v}\underline{v}^t)$ matrix represents the known covariance matrix of the gust disturbance. The remaining covariance matrices in equation (B4) are evaluated as follows.

As a first step toward the determination of J, equation (B2) is expressed in frequency domain form, with the Laplace transform pair to be used defined as follows:

$$\Phi(s) = \frac{1}{\pi}\int_{-\infty}^{\infty}\phi(\tau)e^{-s\tau}\,d\tau \tag{B5}$$

$$\phi(\tau) = \frac{1}{2j}\int_{-j\infty}^{j\infty}\Phi(s)e^{s\tau}\,ds \tag{B6}$$

After taking the Laplace transform of equation (B2), omitting the initial condition terms, and rearranging the remaining terms (ref. 13), one obtains

$$\underline{x}(s) = (Is - D)^{-1} C_V \underline{v}(s) \tag{B7}$$

The term $(Is - D)^{-1}$ consists of a numerator, which is expressed as a matrix whose elements are polynomials in s, divided by a common denominator polynomial obtained from the determinant of $(Is - D)$. Thus the closed-loop poles are the eigenvalues of the matrix D. The numerator polynomials were obtained by the method given in reference 13.

To determine the performance index, statistical averages of the quadratic products of state variables are needed, as well as averages of quadratic products of state and gust disturbance variables. To obtain these averages, the power spectrum of these products is first obtained. The power spectrum that describes the gust disturbance $\underline{v}$ is given in appendix C (eqs. (C6)-(C8)). The resulting spectrum of the state variables and the cross-power spectrum between the state variables and the gust disturbance can be expressed as:

$$\Phi_{xx}(s) = (-Is - D)^{-1} C_V \Phi_{gg}(s) C_V{}^t [(Is - D)^{-1}]^t \tag{B8}$$

$$\Phi_{vx}(s) = \Phi_{gg}(s) C_V{}^t [(Is - D)^{-1}]^t \tag{B9}$$

Since only the cross state-velocity terms are of interest in equation (B9), the $\Phi_{vx}(s)$ matrix can be partitioned into the square matrix $\Phi_{\underline{v}\underline{x}_V}(s)$.

The correlation functions of the variables can be obtained by using the inverse Fourier transform of equations (B8) and (B9). Since only matrices of expected values are needed rather than correlation functions, the integrals to be evaluated by using equation (B6) simplify to

$$E(\underline{x}\underline{x}^t) = \frac{1}{2j} \int_{-j\infty}^{j\infty} \Phi_{xx}(s)\,ds \tag{B10}$$

$$E(\underline{v}\underline{x}_V{}^t) = \frac{1}{2j} \int_{-j\infty}^{j\infty} \Phi_{vx_V}(s)\,ds \tag{B11}$$

Note that the $E(\underline{x}_V \underline{x}_V{}^t)$ matrix (eq. (B4)) is a partitioning of the aircraft velocity state terms in the $E(\underline{x}\underline{x}^t)$ matrix. The integrals were evaluated using the method of residues, in which the residues of the left-half-plane (LHP) poles were evaluated. The result is indicated by

$$E(\underline{x}\underline{x}^t) = \pi \sum_{\text{LHP}} \text{res}\ \Phi_{xx}(s) \tag{B12}$$

$$E(\underline{v}\underline{x}_V{}^t) = \pi \sum_{\text{LHP}} \text{res}\ \Phi_{vx_V}(s) \tag{B13}$$

The matrix of residues that result from each pole is expressed by

$$\text{res } \Phi_{xx}(\gamma_i) = \left[\frac{1}{(n-1)!}\frac{d^{n-1}}{ds^{n-1}}(s-\gamma_i)^n\Phi_{xx}(s)\right]_{s=\gamma_i} \tag{B14}$$

In a similar manner, the residues for the cross covariance terms $E(\underline{v}\underline{x}_v{}^t)$ are obtained from the $\Phi_{vx_v}(s)$ matrix. Hence, the evaluation of equations (B10) and (B11) depends on the form of the closed-loop poles and the disturbance pole. Provision was made in the digital computer program to evaluate the needed combinations of real and complex forms of the nine LHP poles. The gust disturbance was represented by a real double pole (appendix C). For the remaining seven poles, which were obtained from the D matrix representing the closed-loop system, provision was made to evaluate three pole patterns. These patterns were (1) two complex pairs, (2) one complex pair, and (3) one complex pair and a double real pole; the remaining poles in each pattern were simple real.

The performance index (eq. (B4)) was calculated by using the products of the expected values of the covariance matrices determined from equations (B12) and (B13) times the Q and P weighting matrices. Values used for the Q and P matrices in the examples are given in tables 1 and 2.

The method used to evaluate the performance index for a predetermined set of gains is indicated by the equations set forth in this appendix. The set of gains that minimized the performance index was obtained by an iterative process starting with a trial set of gains, as explained in the report.

APPENDIX C

COMPARISON OF TWO GUST DISTURBANCE REPRESENTATIONS

The power spectrum of the gust disturbance selected for the examples is discussed in this appendix. As an aid in this selection, a comparison was made of the system response caused by two commonly used forms of power spectra that represent gust disturbances. The comparison is presented in a general form so that a fairly wide range of conditions is included. Expressions for the elements of the covariance matrix of the response of a system to each of the forms of gust disturbance are obtained first. Results are presented as a ratio of covariances of the response due to each form of the disturbance. The result is shown to be a function of the system poles γ_ℓ and a gust disturbance frequency parameter U_o/L.

The development outlined in the first part of appendix B was used in determining the covariance of the system response. The power spectrum of the system response due to a known input spectrum was indicated by the matrix equation (B8).

$$\Phi_{xx}(s) = (-Is - D)^{-1} C_v \Phi_{gg}(s) C_v{}^t [(Is - D)^{-1}]^t \tag{C1}$$

The gust disturbance matrix Φ_{gg} is assumed to be in diagonal form.

To illustrate effects of the form of the disturbances, the terms in equation (C1) are first rearranged as follows. Each element of the matrix $\Phi_{xx}(s)$ can be expressed as a sum of the components of the gust disturbance.

$$\Phi_{ij}(s) = \sum_k \frac{N_{ijk}(s)}{d(s)d(-s)} \Phi_{g_k g_k}(s) \tag{C2}$$

where $N_{ijk}(s)$ is a polynomial in s and $d(s) = \det(Is - D)$.

Each term in the expansion in equation (C2), which results from a single disturbance element k, can be rearranged by a partial fraction expansion into the following form:

$$\Phi_{ijk}(s) = \sum_\ell |\gamma_\ell|^2 \left(\frac{F_{ijk\ell} + G_{ijk\ell} s}{\gamma_\ell{}^2 - s^2} \right) \Phi_{g_k g_k}(s) \tag{C3}$$

where γ_ℓ is an eigenvalue of the matrix D. The constants F and G are generally complex if γ_ℓ is complex. For the discussion in this appendix, the eigenvalues are assumed to be distinct.

An element of the covariance matrix due to the kth element of the gust disturbance $E_k(x_i x_j)$ can be obtained from the expression for the power spectrum by using equation (B10). The contribution to an element of the covariance matrix due to a single term of the expansion of equation (C3) is

$$E_{k\ell}(x_i x_j) = \frac{1}{2j} \int_{j\infty}^{j\infty} \Phi_{ijk\ell}(s)ds$$

$$= \frac{|\gamma_\ell|^2}{2j} \int_{-j\infty}^{j\infty} \left(\frac{F_{ijk\ell} + G_{ijk\ell} s}{\gamma_\ell^2 - s^2} \right) \Phi_{g_k g_k}(s)ds \qquad \text{(C4)}$$

Note that if complex conjugate eigenvalues are present, the constants F and G will occur as complex conjugate pairs. Hence, only the real part of the expression need be evaluated. Furthermore, since the disturbance spectra $\Phi_{g_k g_k}$ are even functions of s, the constant G will not contribute to the integral. Hence, equation (C4) can be expressed as

$$E_{k\ell}(x_i x_j) = \mathcal{R}\left[\frac{F_{ijk\ell}|\gamma_\ell|^2}{2j} \int_{-j\infty}^{j\infty} \frac{1}{\gamma_\ell^2 - s^2} \Phi_{g_k g_k}(s)ds \right] \qquad \text{(C5)}$$

The power spectra used to represent the horizontal and vertical components of gust velocity are arranged in the following matrix form.

$$\Phi_{gg} = \begin{bmatrix} \Phi_{uu} & 0 \\ 0 & \Phi_{ww} \end{bmatrix} \qquad \text{(C6)}$$

The equations for the components, obtained from reference 8, are expressed in terms of the time transform variable s rather than the spatial transform variable $j\Omega$ used in the reference. For the Dryden form, which is a rational function of the variable s, the spectra for the velocities parallel and perpendicular to the direction of motion are

$$\Phi_{uu} = \frac{2L_u \sigma_{u_g}^2}{U_o \pi} \frac{1}{[1 - (L_u/U_o)^2 s^2]} \qquad \text{(C7)}$$

and

$$\Phi_{ww} = \frac{L_w \sigma_{w_g}^2}{U_o \pi} \frac{\left\{1 - 3[(L_w/U_o)s]^2\right\}}{\left\{1 - [(L_w/U_o)s]^2\right\}^2} \tag{C8}$$

For the Von Kármán form, which is an irrational function of the variable s, the spectra for the longitudinal and vertical velocities are

$$\Phi_{uu} = \frac{2L_u \sigma_{u_g}^2}{U_o \pi} \frac{1}{\left\{1 - [1.339(L_u/U_o)s]^2\right\}^{5/6}} \tag{C9}$$

and

$$\Phi_{ww} = \frac{L_w \sigma_{w_g}^2}{U_o \pi} \frac{\{1 - (8/3)[1.339(L_w/U_o)s]^2\}}{\{1 - [1.339(L_w/U_o)s]^2\}^{11/6}} \tag{C10}$$

The effects of the two longitudinal spectra are compared first. For the rational case, the contribution of the eigenvalue γ_ℓ to an element of the covariance matrix can be obtained by the substitution of equation (C7) into equation (C5).

$$\frac{E_{u\ell}^{rat}}{\sigma_{u_g}^2}(x_i x_j) = \Re\left(\frac{F_{iju\ell} L_u |\gamma_\ell|^2}{\pi j U_o} \int_{-j\infty}^{j\infty} \frac{ds}{(\gamma_\ell^2 - s^2)\{1 - [(L_u/U_o)s]^2\}}\right) \tag{C11}$$

where the superscript "rat" denotes a result due to a rational form of gust disturbance. The integral can be evaluated by a contour integration, which is expressed by $2\pi j$ times the sum of the residues of the LHP poles. The integral becomes

$$\frac{E_{u\ell}^{rat}}{\sigma_{u_g}^2}(x_i x_j) = \Re\left[\frac{F_{iju\ell}}{e^{j\mu_\ell}(e^{j\mu_\ell} + K_{\ell_u})}\right] \tag{C12}$$

where

$$\mu_\ell = \tan^{-1}\left|\frac{\text{imag. part } \gamma_\ell}{\text{real part } \gamma_\ell}\right| \tag{C13}$$

$$K_{\ell_u} = \frac{U_o}{|\gamma_\ell| L_u} \tag{C14}$$

Note that $\cos \mu_\ell = \zeta_\ell$. For real γ_ℓ, equation (C12) reduces to

$$\frac{E_{u\ell}^{rat}(x_i x_j)}{\sigma_{u_g}^2} = \frac{F_{iju\ell}}{1 + k_{\ell_u}} \tag{C15}$$

For the irrational longitudinal case, a comparable expression for equation (C12) is obtained by the substitution of equation (C9) into equation (C5), with $s = (U_o/L)j\omega$ and with the definitions of μ and K_{ℓ_u} given by equations (C13) and (C14).

$$\frac{E_{u\ell}^{irr}(x_i x_j)}{\sigma_{u_g}^2} = \Re\left\{\frac{2F_{iju\ell}}{\pi}\int_o^\infty \left[e^{2j\mu_\ell} + (K_{\ell_u}\omega)^2\right][1 + (1.339\omega)^2]^{5/6}\right\} \tag{C16}$$

where the superscript "irr" denotes a result due to the irrational form of gust disturbance. After a trignometric substitution to make the integration limits finite, the integral was evaluated numerically by means of Simpson's rule. A useful comparison between the relative effects of the two forms of gust representation of the expected values of the response can be obtained from the function obtained by dividing equation (C16) by equation (C12) and neglecting the effect of the "real part" operator on the ratio of the complex expression.

$$K_u = \frac{2e^{j\mu_\ell}\left(e^{j\mu_\ell} + K_{\ell_u}\right)}{\pi}\left\{\int_o^\infty \left[e^{2j\mu_\ell} + (K_{\ell_u}\omega)^2\right][1 + (1.339\omega)^2]^{5/6}\right\} \tag{C17}$$

This simplification forms a valid comparison for most cases since the phase difference between the two complex functions (eqs. (C12) and (C16)) is generally small. A useful property of the expression is that it approaches unity for both very large and small values of the frequency variable K_{ℓ_u}.

Results for the transverse gust disturbance are obtained in a similar manner. For the rational Dryden form, the expression to be integrated is obtained by the substitution of equation (C8) into equation (C5):

$$\frac{E_{w\ell}^{rat}}{\sigma_{w_g}^2}(x_i x_j) = \Re\left(\frac{F_{iju\ell}L_w|\gamma_\ell|^2}{2\pi j U_o}\int_{-j\infty}^{j\infty} \frac{\{1 - 3[(L_w/U_o)s]^2\}ds}{(\gamma_\ell^2 - s^2)\{1 - [(L_w/U_o)/s]^2\}^2}\right) \tag{C18}$$

where

$$K_{\ell_W} = \frac{U_o}{|\gamma_\ell| L_W} \tag{C19}$$

The integral was evaluated by the method of residues to obtain the following expression for the contribution to an element of the covariance matrix.

$$\frac{E^{rat}_{w\ell}}{\sigma^2_{wg}}(x_i x_j) = \Re\left[\frac{F_{ijw\ell}\left(K_{\ell_W} e^{-j\mu_\ell} + 2\right)}{2\left(K_{\ell_W} + e^{j\mu_\ell}\right)^2}\right] \tag{C20}$$

The resulting expression for the irrational transverse gust velocity is, with $s = (U_o/L)j\omega$,

$$\frac{E^{irr}_{w\ell}}{\sigma^2_{wg}}(x_i x_j) = \Re\left\{\frac{F_{ijw\ell}}{\pi}\int_o^\infty \frac{[1 + (8/3)(1.339\omega)^2]d\omega}{\left[e^{2j\mu_\ell} + (K_{\ell_W}\omega)^2\right][1 + (1.339\omega)^2]^{11/6}}\right\} \tag{C21}$$

The equation used for the ratio of transverse disturbance functions is obtained by dividing equation (C21) by equation (C20) and neglecting the effect of the "real part" operator.

$$K_W = \frac{2\left(K_{\ell_W} + e^{j\mu_\ell}\right)^2}{\pi\left(K_{\ell_W} e^{-j\mu_\ell} + 2\right)}\int_o^\infty \frac{[1 + (8/3)(1.339\omega)^2]d\omega}{\left[e^{2j\mu_\ell} + (K_{\ell_W}\omega)^2\right][1 + (1.339\omega)^2]^{11/6}} \tag{C22}$$

Values of the ratios of effects of rational and irrational gust disturbances on expected values of system response for longitudinal (eq. (C17)) and transverse (eq. (C22)) disturbances are shown in figure 10. Values of the eigenvalue damping parameter μ_ℓ of 0° and 60° are indicated. The zero value represents the real eigenvalue case ($\zeta = 1.0$) while the 60° value ($\zeta = 0.5$) represents an upper limit on the range of dimensionless damping of most interest for controlled systems. As was desired, the amplitude curves are seen to approach unity for both the very low and high frequency ranges of the frequency ratio parameter K_ℓ. Curves of the phase differences are shown to demonstrate the accuracy of the assumption made in neglecting the effect of the "real part" operator on the K_u and K_W expressions. Since these angles are quite small, the assumption is validated. The greatest change in the amplitude curves occurs in the frequency range where the gust frequency is one-third to one-half of the system frequency. However, the overall difference in effects of the two forms of

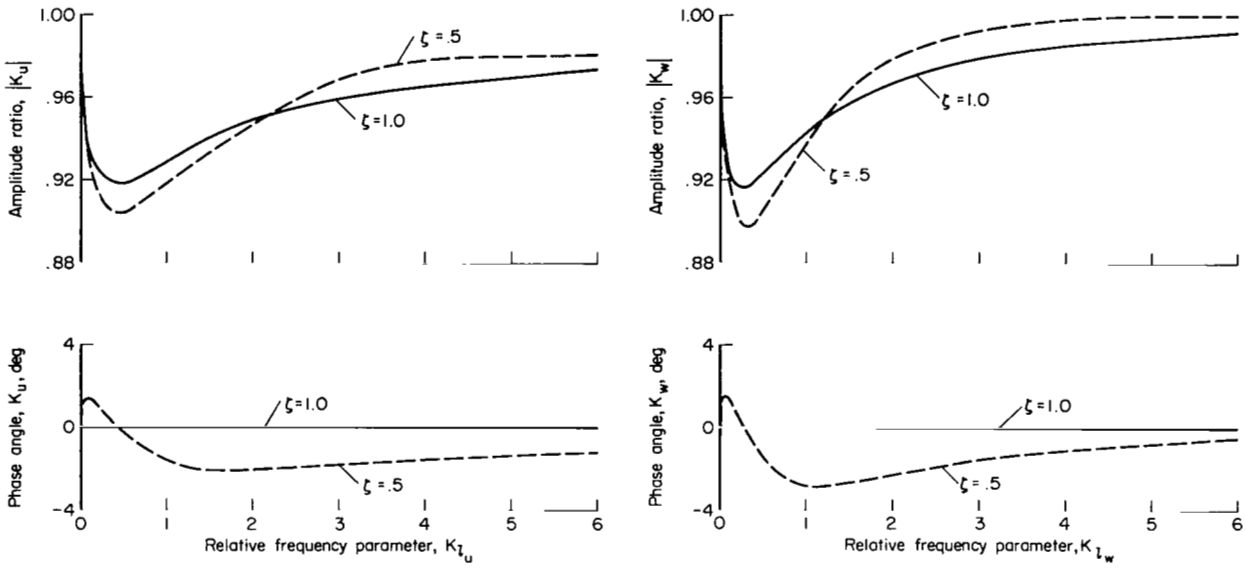

(a) Longitudinal gust ratio, K_u.

(b) Transverse gust ratio, K_w.

Figure 10.– Comparison of system response to Dryden and Von Kármán forms of gust disturbances.

disturbances is seen to be quite small for both the longitudinal and transverse cases. Because of these small differences, the more convenient Dryden form (eqs. (C7) and (C8)) is used for the examples in the report. It may be noted, however, that the expressions for K_u and K_w could provide a means for modifying results based on the Dryden form of disturbance to those based on the Von Kármán form when a residue method of computation is used.

The power spectra are assumed to be valid for the representation of variations of gust velocities specified in the stability axis system (appendix A) rather than the fixed axis system used in reference 8. This approximation is valid since deviations from the nominal constant glide-slope flight path are assumed to be small. The gust parameters selected for the low altitude range of interest are based on results given in reference 9. Gust scale lengths of 400 ft for the vertical gusts and 600 ft for the longitudinal gusts were selected. The relative rms magnitude of the two gust components was $\sigma_{u_g}/\sigma_{w_g} = \sqrt{3}/2$.

REFERENCES

1. Gorham, J. A.; Richter, H. K.; and Lee, F. B.: Where Are We Now With All-Weather Landing? AIAA Paper 67-572, presented at AIAA Guidance, Control and Flight Dynamics Conference, August 14-16, 1967.

2. Kalman, R. E.; and Englar, T.: Fundamental Study of Adaptive Control Systems. Volumes I and II. ASD-TR-61-27, March 1961 and March 1962.

3. Rynaski, E. G.; and Whitbeck, R. F.: The Theory and Application of Linear Optimal Control. Air Force Flight Dynamics Lab. Rep. AFFDL-TR-65-28, 1965.

4. Rynaski, E. G.; Whitbeck, R. F.; and Wierwille, W. W.: Optimal Control of a Flexible Launch Vehicle. Cal. Rep. IH-2089-F-1, July 1966.

5. Whitbeck, R. F.: A Frequency Domain Approach to Linear Optimal Control. J. Aircraft, vol. 5, no. 4, July-August 1968, pp. 395-401.

6. Cooper, George E.; and Harper, Robert P.: The Use of Pilot Rating in the Evaluation of Aircraft Handling Qualities. NASA TN D-5153, 1969.

7. Hague, D. S.; and Glatt, C. R.: A Guide to the Automated Engineering and Scientific Optimization Program – AESOP. NASA CR-73201, 1968

8. Houbolt, J. C.; Steiner, R.; and Pratt, K. G.: Dynamic Response of Airplane to Atmospheric Turbulence Including Flight Data on Input and Response. NASA TR R-199, 1964.

9. Gunter, D. E.; Jones, C. W.; Jones, J. W.; and Monson, K. R.: Low Altitude Atmospheric Turbulence Lo-Locat Phases I and II. ASD-TR-69-12, February 1969.

10. Anon.: Criteria for Approval of Category II Landing Weather Minima. FAA AC No. 120-20, June 6, 1966.

11. Anon.: Dynamics of the Airframe. Northrop Aircraft, Inc., BuAer Rep. AE-61-4, Vol. II, Sept. 1952.

12. Etkin, B.: Dynamics of Flight. John Wiley & Sons, New York, 1959, pp. 310-320.

13. Zadeh, L. A.; and Dosoer, C. A.: Linear System Theory. Ch. 5, McGraw-Hill Book Co., N. Y., 1963.

TABLE 1.- AIRCRAFT AND CONTROL SYSTEM PARAMETERS FOR SUBSONIC TRANSPORT

(a) Performance criterion parameters

Gain constraints, K_{max} and $K_{V_{max}}$

Control variables	Feedback variables								
	u, ft/sec	θ, rad	$\dot{\theta}$, rad/sec	w/U_o, rad	h, ft	δ_e	δ_t	$u - u_g$, ft/sec	$(w - w_g)/U_o$, rad
u_{δ_e}, rad	0	|10|	|15|	|10|	|0.015|	0	0	0	|10|
u_{δ_t}, 1000 lb	0	|50|	0	|50|	|0.15|	0	0	|0.2|	|50|

Pole constraints:

$\zeta_{\ell im} = 0.6$, $\Re_{\ell im} = -0.04$ sec^{-1}

Performance index:

$$J = 2u^2 + h^2 + 10{,}000\delta_e^2 + 10\delta_t^2 + \frac{1000(w - w_g)^2}{U_o^2(\alpha_o - \alpha_s)^2}$$

(b) Aircraft parameters - landing gear and flaps extended

C_{L_α}	5.22 rad^{-1}	M_{δ_t}	1.025×10^{-3} rad/sec^2 kilo-lb
$C_{L_{\dot{\alpha}}}$	1.32 rad^{-1}	X_{δ_t}	0.1612 ft / sec^2 kilo-lb
C_{L_q}	7.68 rad^{-1}	Z_{δ_t}	-8.85×10^{-3} ft/sec^2 kilo-lb
$C_{L_{\delta_e}}$	0.302 rad^{-1}	α_s	0.25 rad
C_{m_α}	-1.062 rad^{-1}	γ_o	-3.0°
$C_{m_{\dot{\alpha}}}$	-4.01 rad^{-1}	ρ	0.002378 slug/ft^3
C_{m_q}	-12.3 rad^{-1}	τ_e	0.0833 sec
$C_{m_{\delta_e}}$	-0.923 rad^{-1}	τ_t	0.8 sec
c	22.16 ft	m	6210 slugs
I_y	3.9×10^6 slug-ft^2	S	2758 ft^2

TABLE 1.- AIRCRAFT AND CONTROL SYSTEM PARAMETERS FOR SUBSONIC TRANSPORT - Concluded

(c) Aircraft parameters that vary with steady-state forward velocity

U_o, knots	107	120	130	145
C_{D_o}	0.250	0.185	0.151	0.121
C_{D_α}, rad^{-1}	.922	.782	.699	.605
C_{L_o}	1.840	1.468	1.250	1.002
C_{m_o}	-.0275	-.0219	-.0181	-.0145
α_o, rad	.201	.125	.080	.029

TABLE 2.- AIRCRAFT AND CONTROL SYSTEM PARAMETERS FOR SUPERSONIC TRANSPORT

(a) Control system parameters

Gain constraints, K_{max} and $K_{V_{max}}$

Control variables	Feedback variables									
	u, ft/sec	θ, rad	$\dot{\theta}$, rad/sec	w/U_o, rad	h, ft	δ_e	δ_t	$u - u_g$, ft/sec	$(w - w_g)/U_o$, rad
δ_e, rad	0	|15|	|22|	|15|	|0.022|	0	0	0	|15|
δ_t, 1000 lb	0	|150|	0	|150|	|.45|	0	0	|0.6|	|150|

Pole constraints:

$$\zeta_{\ell im} = 0.6 , \qquad \Re_{\ell im} = -0.04 \text{ sec}^{-1}$$

Performance index:

$$J = 2u^2 + h^2 + 4500\delta_e^2 + 2\delta_t^2 + \frac{1000(w - w_g)^2}{U_o^2(\alpha_o - \alpha_s)^2}$$

(b) Aircraft parameters - landing gear and flaps extended

C_{D_o}	0.113	U_o	145 knots
C_{D_α}	0.29 rad^{-1}	M_{δ_t}	1.49×10^{-4} rad/sec^2 kilo-lb
C_{L_o}	0.615	X_{δ_t}	0.0845 rad / sec^2 kilo-lb
C_{L_α}	3.15 rad^{-1}	Z_{δ_t}	-1.28×10^{-3} ft/sec^2 kilo-lb
$C_{L_{\dot{\alpha}}}$	0.2 rad^{-1}	c	158.1 ft
C_{L_q}	1.0 rad^{-1}	I_y	40.2×10^6 slug-ft^2
$C_{L_{\delta_e}}$	0.132 rad^{-1}	m	11,830 slugs
		S	9,000 ft^2
C_{m_o}	-0.0031	α_o	0.171 rad
C_{m_α}	-0.0430 rad^{-1}	α_s	0.332 rad
$C_{m_{\dot{\alpha}}}$	-0.10 rad^{-1}	γ_o	-3.0°
		ρ	0.002378 slug/ft^3
C_{m_q}	-0.33 rad^{-1}	τ_e	0.10 sec
$C_{m_{\delta_e}}$	-0.0363 rad^{-1}	τ_t	1.0 sec

TABLE 3.- SYSTEM ERRORS AND CONTROL GAINS FOR OPTIMIZED SYSTEM FOR SUBSONIC TRANSPORT

[Approach velocity = 132 knots, $\sigma_{u_g} = \sqrt{3/2}$ fps, $\sigma_{w_g} = 1$ fps]

Expected values	Form of vertical velocity feedback		
	Inertial vertical velocity feedback	Barometric vertical velocity feedback	No vertical velocity feedback
u^2, $(fps)^2$	0.35	0.23	0.28
θ^2, $rad^2 \times 10^5$	2.1	1.4	.9
$\dot{\theta}^2$, $(rad/sec)^2 \times 10^5$	.84	.37	.08
$(w/U_o)^2 \times 10^5$	3.0	2.3	1.8
h^2, ft^2	1.1	4.7	7.1
δ_e^2, $rad^2 \times 10^5$	1.4	4.9	2.0
δ_t^2, $(kilo\text{-}lb)^2$	.14	.14	.13
$(1/U_o^2)(w - w_g)^2 \times 10^5$	2.4	2.6	2.0
$\dot{h}^2$, $(fps)^2$	.24	.64	.61
J	4.2	8.0	10.1
Gust rms, σ_g, for σ_h = 6 ft tolerance, fps	5.7	2.8	2.2
Gains			
$k_{\delta_e \theta}$	-10.0	-10.0	-10.0
$k_{\delta_e \dot{\theta}}$	-3.0	-3.3	-3.9
$k_{\delta_e (w/U_o)}$	6.2	2.5	0
$k_{\delta_e h}$, rad/ft	-.015	-.015	-.012
$k_{\delta_t \theta}$, kilo-lb/rad	-20	-20	-50
$k_{\delta_t (w/U_o)}$, kilo-lb	-10	25	0
$k_{\delta_t h}$, kilo-lb/ft	.15	.15	.06
$k_{\delta_t (u - u_g)}$, kilo-lb/fps	.12	.12	.16

Table 4.- COMPARISON OF PERFORMANCE OF SUBSONIC AND SUPERSONIC TRANSPORTS

[Approach velocity = 145 knots]

Form of vertical velocity feedback	Subsonic transport		Supersonic transport	
	$E(J)/\sigma_g^2$, sec^2	$E(h^2)/\sigma_g^2$, sec^2	$E(J)/\sigma_g^2$, sec^2	$E(h^2)/\sigma_g^2$, sec^2
Inertial vertical velocity feedback	2.9	0.8	7.1	4.3
No vertical velocity feedback	7.2	5.0	9.1	6.5
Barometric vertical velocity feedback	6.1	3.3	8.9	5.9
Inertial plus barometric vertical velocity feedback	2.6	.7	6.2	2.8

TABLE 5.- EFFECT OF FORM OF GUST DISTURBANCE ON SUPERSONIC TRANSPORT

[Inertial vertical velocity feedback, approach velocity = 145 knots]

Form of gust disturbance	E(J)	$E(h^2)$, ft^2	L_u, ft	L_w, ft	σ_u, fps	σ_w, fps
Vertical	4.6	3.5		400	0	1
Horizontal	2.5	.8	600		$\sqrt{3/2}$	0
Vertical	2.7	1.8		200	0	1
Horizontal	1.8	.6	300		$\sqrt{3/2}$	0
Vertical but with horizontal spectral form	5.7	3.9		(400)(2/3)	0	1

NASA-Langley, 1971 — 21 A-3244

"The aeronautical and space activities of the United States shall be conducted so as to contribute . . . to the expansion of human knowledge of phenomena in the atmosphere and space. The Administration shall provide for the widest practicable and appropriate dissemination of information concerning its activities and the results thereof."

—NATIONAL AERONAUTICS AND SPACE ACT OF 1958

NASA SCIENTIFIC AND TECHNICAL PUBLICATIONS

TECHNICAL REPORTS: Scientific and technical information considered important, complete, and a lasting contribution to existing knowledge.

TECHNICAL NOTES: Information less broad in scope but nevertheless of importance as a contribution to existing knowledge.

TECHNICAL MEMORANDUMS: Information receiving limited distribution because of preliminary data, security classification, or other reasons.

CONTRACTOR REPORTS: Scientific and technical information generated under a NASA contract or grant and considered an important contribution to existing knowledge.

TECHNICAL TRANSLATIONS: Information published in a foreign language considered to merit NASA distribution in English.

SPECIAL PUBLICATIONS: Information derived from or of value to NASA activities. Publications include conference proceedings, monographs, data compilations, handbooks, sourcebooks, and special bibliographies.

TECHNOLOGY UTILIZATION PUBLICATIONS: Information on technology used by NASA that may be of particular interest in commercial and other non-aerospace applications. Publications include Tech Briefs, Technology Utilization Reports and Technology Surveys.

Details on the availability of these publications may be obtained from:

SCIENTIFIC AND TECHNICAL INFORMATION OFFICE

NATIONAL AERONAUTICS AND SPACE ADMINISTRATION

Washington, D.C. 20546